The role of binary pulsars in testing gravity theories

Andrea Possenti and Marta Burgay

Abstract Radio pulsars are neutron stars (NSs) which emit collimated beams of radio waves, observed as pulses, once per rotation of the neutron star. A subgroup of the radio pulsars behave as highly stable clocks and monitoring the times of arrival of their radio pulses can provide an accurate determination of their positional, rotational and orbital parameters, as well as indications on the properties of their space-time environment. In this chapter we focus on the so-called relativistic binary pulsars, recycled neutron stars orbiting around a compact companion star. Some of them can be used as unique tools to test General Relativity and other gravitational theories. The methodology for exploiting these sources as laboratories for gravity theories is first explained and then some of the most relevant recent results are reviewed.

1 The many faces of pulsar science

Pulsars are radio sources representing a paradigm for the aims and the procedures of the modern astrophysics. In fact, on one side, they are very intriguing celestial objects *per se*, whereas, on another side, they can be exploited as unique tools for investigating the behavior of Nature and constraining its most fundamental laws.

As to the former aspect, the investigation of the radio pulsars (i.e. highly magnetized and rapidly spinning neutron stars) is for example an important ingredient for understanding the final fate of the massive stars, as well as for clarifying the processes occurring in the evolution of binary systems involving at least one compact

Andrea Possenti
INAF-Osservatorio Astronomico di Cagliari, via della Scienza 5, 09047 Selargius (CA), (Italy),
e-mail: possenti@oa-cagliari.inaf.it

Marta Burgay
INAF-Osservatorio Astronomico di Cagliari, via della Scienza 5, 09047 Selargius (CA), (Italy),
e-mail: burgay@oa-cagliari.inaf.it

star. The explanation of the broadband emission of electromagnetic waves (from the radio to the GeV and TeV bands) has been representing a challenging task for generations of experts of electrodynamics, while the expected emission of accelerated particles impacts on the studies of the cosmic rays. Also, the dispersion of the pulsed signal while it goes across the interstellar medium opens the possibility of determining the distribution of the free electrons in the Milky Way (e.g. [1]), and the observation of the Faraday rotation of the polarized signals helps in mapping the large-scale structure of the Galactic magnetic field (e.g. [2]). Furthermore, when discovered in a globular cluster, the pulsars provide a way for studying the cluster's dynamics and potential well, potentially unveiling the presence of non luminous matter in the form of black-holes [3].

Looking at the second aspect, the study of the pulsars is of utmost relevance for investigating two of the fundamental *"forces"* in Nature, the nuclear interaction and the gravitational interaction. No terrestrial laboratory can compress a sizable amount of matter to nuclear density; hence the equation of state for the nuclear matter at ultra high density can only be investigated in a neutron star, where Nature provides matter experiencing those extreme conditions. In particular, each equation of state for the nuclear matter predicts a precise value for the radius and for the moment of inertia of a neutron star, depending on the gravitational mass (below a maximum mass) and the rotational frequency (below a maximum frequency) of the star. The maximum allowed mass and frequency are also dependent on the equation of state. The observation of the very high spin rate [4] and/or of the high mass of some pulsars [5, 6] has already been used for constraining the equation of state for the nuclear matter. The measurement of the moment of inertia is a more difficult task, but it might be attained in the near future for some particularly favorable pulsar (i.e. the Double pulsar [7]).

This chapter mostly deals with the application of the pulsars to the investigation of the gravitational theories. We will first briefly summarize the rudiments of pulsar science (§ 2), and the evolutionary scenario leading to the formation of the the so-called *relativistic binary pulsars*. Then, in § 3 the principles and methodology of the pulsar timing will be reviewed and the most interesting applications presented in § 4. Last section 5 will illustrate where this field of research is heading to.

2 Rudiments for pulsars' investigators

Pulsars are celestial objects which only progessivly unveil their parameters. The peculiarities and/or the degree of scientific interest of a new source only emerges after having undertaken a patient monitoring of its radio signal, over timescales starting from few weeks and sometimes reaching few decades. One of the basic parameters is the spin period first derivative, $\dot{P}$, a determination of which typically requires almost one year of regular observations (see § 3).

Assuming that the emission is due to the rotational energy loss in the form of magneto-dipole radiation (see eq. 1), its measurement allows us to estimate im-

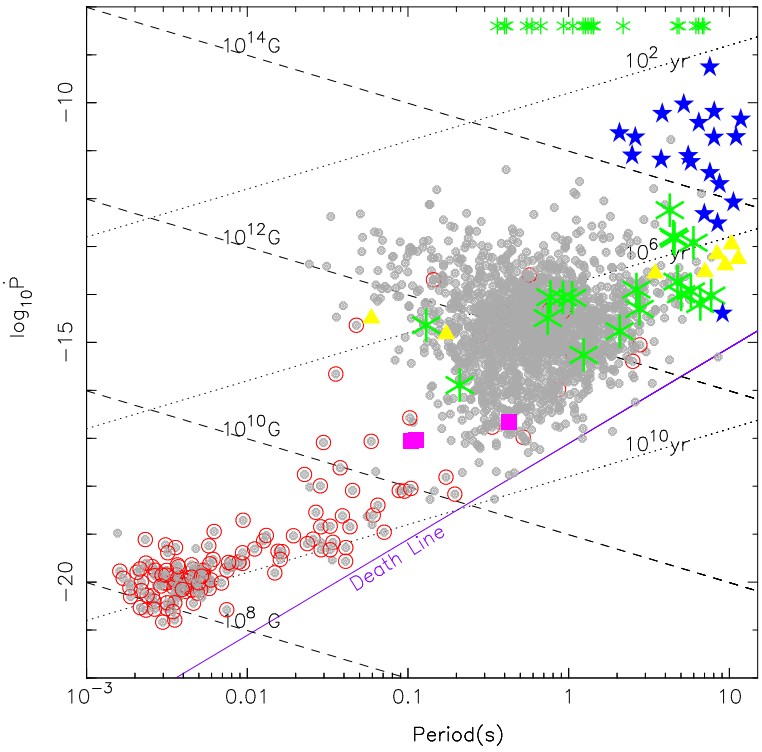

Fig. 1 Period-period derivative diagram. Grey dots are Galactic field radio pulsars (those surrounded by a red circle being in a binary system); purple squares are X-ray Dim Isolated NS (XDINSs; e.g. [8]); yellow triangles are Central Compact Objects (CCOs; e.g. [9]); green asterisks are Rotating Radio Transients (RRATs; the top smaller ones do not have yet a measured $\dot{P}$; e.g. [10]); blue stars are magnetars [11]. Dashed lines denote equal dipolar magnetic field, calculated as in equation 2, while dotted ones are equal spin-down age (eq. 3) lines. The violet line is the so-called *death line* (in particular the *death-line C* of [12]) for values of P and $\dot{P}$ below which the mechanism responsible for radio emission is not efficient anymore and the pulsar switches off. We point out that the use of a specific line is only for the sake of simplicity; a death valley [12], across which the pulsars' signal slowly fades out in time, should better replace a single line. Data taken [13] from [14] and [15].

portant physical parameters such as the dipolar surface magnetic field B_s and the spin-down age of the pulsar. The basic equation is:

$$-I_{NS}\omega\dot{\omega} = \frac{2}{3}\frac{1}{c^3}\omega^4 B_s^2 R_{NS}^6 \sin^2\alpha \tag{1}$$

where I_{NS} is the moment of inertia of the neutron star (NS), $\omega = 2\pi/P$ its angular velocity, R_{NS} its radius and α the angle between the rotation and the magnetic axes. Expressing eq. 1 in terms of the spin period, assuming $\alpha = 90^\circ$, and using the standard values for $I_{NS} = 10^{45}$ g cm^2 and $R_{NS} = 10^6$ cm, we can derive an estimate of

the surface dipolar magnetic field at the magnetic equator as:

$$B_s = 3.2 \times 10^{19} \sqrt{P\dot{P}} \qquad \mathrm{G} \tag{2}$$

and, after integration of the differential equation in time, we can calculate the so-called spin-down age (or characteristic age) of the pulsar as:

$$\tau_c = \frac{P}{2\dot{P}} \left(1 - \frac{P_0^2}{P^2} \right) \sim \frac{P}{2\dot{P}} \tag{3}$$

where P_0 is the initial spin period of the pulsar, usually considered negligible with respect to the current one (whence the last approximation in equation 3).

According to [14, 13] more than 2000 radio pulsars have been discovered in the field of our Galaxy, in the Galactic globular clusters and in the Magellanic Clouds. The most interesting of which are the so-called *millisecond* or, better saying *recycled* pulsars (see later) located in the bottom-left corner of the $P - \dot{P}$ diagram of Figure 1, whose short pulse duration and particularly regular pulsations are very helpful to study the many physical and astrophysical problems listed in § 1.

2.1 Basics of evolution

According to the current paradigm, the recycled pulsars, to which the relativistic binaries belong, are believed to be formed in binary systems in which the companion star, during its evolution, transfers matter and angular momentum, via wind or Roche lobe overflow, onto the neutron star surface (*recycling model*) [16]. The NS is hence spun-up to periods of the order of few or few tens of milliseconds, depending on the amount of matter accreted, which, in turn, depends on the initial mass of the companion.

The initial mass of the companion star, as well as the orbital separation at the time of formation of the NS, leads to very different evolutionary paths for the binary, whose in-depth description goes beyond the scope of this chapter. For a thorough discussion of (some of) the different possible evolutionary paths of binary pulsars the reader can rely on the review [17], or on [18] for the case of the evolution of the increasing number of double neutron stars, as well as [19] for the case of the evolution of binaries in globular clusters.

A sketch in the $P - B_s$ diagram of the two evolutionary paths which are most relevant for the relativistic binaries is displayed in Fig. 2. At birth, the NS spins fast (tens of ms) and has a high magnetic field ($10^{11 \div 13}$ G), hence a high $\dot{P}$. Therefore the pulsar slows down in a relatively short time scale moving left in the diagram. It is still debated whether a significant spontaneous decay of the surface magnetic field occurs [20] or does not [21] during this stage. When the death-valley (a region surrounding the nominal model-dependent death-line) is crossed, the pulsar

switches off. If the NS is isolated it ends its electromagnetic life in the so-called pulsar graveyard.

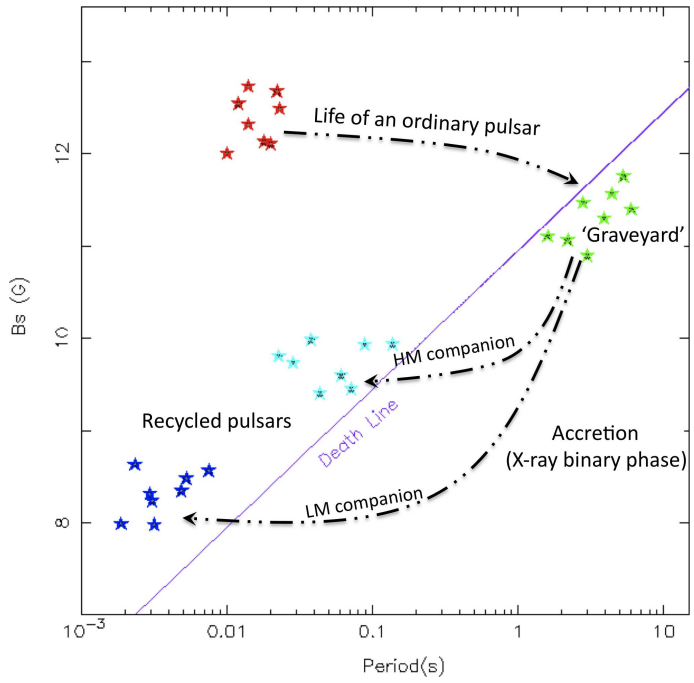

Fig. 2 Spin evolution of a neutron star in the period - magnetic field diagram (analogous to the $P - \dot{P}$ diagram and obtained using eq. 2).

If the progenitor of the pulsar companion is a star more massive than 8-10 $M_\odot$ and the orbital separation is suitable, a phase of mass transfer from the companion can establish, followed by a phase of common envelope, during which the two stars are included in the material lost by the companion and during which the orbit shrinks. Since the evolution of a massive star is relatively fast, the amount of transferred matter, hence of angular momentum, is small. The massive star ends its life in a supernova explosion leaving behind, under favorable circumstances, a binary system containing two neutron stars, i.e. a so-called Double Neutron Star (DNS) binary. Due to the effect of the second supernova, the binary acquires a high eccentricity. The first born NS is a so-called *mildly recycled* pulsar, spun-up to tens of milliseconds and typically brought back above the death-line: in fact the short duration of the accretion phase also decreases the surface magnetic field of a couple of orders of magnitude only, thus leaving a NS with $B_s \sim 10^{10}$ G. The second born NS behaves as a young radio pulsar, slowing-down rapidly and reaching the death-line much faster than the mildly recycled pulsar. This path is labeled as "HM companion" in Fig. 2.

Among the known pulsars with a high mass companion, 10 have a neutron star companion. Sorted according to Right Ascension (RA), they are: J0737−3039A [22] and J0737−3039B [23], composing the first (and so far the only) known double pulsar system (this will be described in details in section 4.2.2); J1518+4904 [24]; J1537+1151 (better known as B1534+12 and described in section 4.2.1) [25, 26], the only other DNS besides the double pulsar for which all 5 post-Keplerian parameters have been measured; J1756−2251 [27]; J1811−1736 [28, 29]; J1829+2456 [30]; J1906+0746 [31], whose undetected companion is likely the recycled pulsar in the system; J1915+1606 (better known as B1913+16, see section 4.2.1), the first known binary pulsar whose discoverers were awarded with the Nobel prize for physics in 1993 [32, 33] and J2129+1210C in the globular cluster M15 [34, 35].

If the progenitor of the pulsar companion has a small mass, below ~ 8 $M_\odot$, its evolution is slower. When the companion star expands due to its nuclear evolution, it fills its Roche lobe starting to transfer mass through the inner Lagrangian point. The mass transfer phase lasts up to $\sim 10^8$ years, during which the mass accreted onto the NS surface is able to accelerate the NS up to few milliseconds, to 'bury' the NS surface magnetic field down to $\sim 10^8 \div 10^9$ G and to circularize the orbit. Once the accretion stops, the NS is again above the death line and is able to shine as a *fully recycled* millisecond pulsar. The companion, not having an initial mass high enough to ignite a supernova explosion, typically ends quietly its life as a white dwarf (WD) in an almost circular orbit. This evolutionary path is labeled as "LM companion" in Fig. 2.

The sample of the pulsars with a low mass companion (in most cases a NS–WD system) is larger than the sample of DNS binaries. In a dozen of these systems some relativistic effects has been already observed. Two remarkable cases are that of J1614−2230 and of J0348+0432. For the former, the determination of both the post-Keplerian parameters related to the Shapiro delay led to determine that the neutron star has a mass very close to 2 solar masses (1.97 ± 0.04 $M_\odot$ with a companion mass of 0.5 $M_\odot$, [5]). The masses of the two stars were separately measured with high precision (2.01 ± 0.04 $M_\odot$ for the pulsar and 0.172 ± 0.003 $M_\odot$ for the white dwarf [6]) also in the second binary, by combining the determination of the post-Keplerian parameter related to the decay of the orbit of the neutron star with the phase-resolved optical spectroscopy of its white-dwarf companion. These are the highest neutron star masses measured with such accuracy to date. That constrains the equation of state for the nuclear matter, effectively ruling out the softest equations of state. In the framework of the study of the gravity theories, another very interesting binary of this class is J1738+0333, which is providing at the moment the most stringent test to the class of the scalar-tensor gravity theories [36, 37] (see section 4.2.3).

In effect, the masses of the companion star in NS–WD systems, span a large range from 0.02 $M_\odot$ (typically Helium WDs) to ~ 1 $M_\odot$ (typically Carbon-Oxygen WDs). As we will show in section 4.2.3, the often comparable masses (but very different radius) of the two stars in these systems can make them a better target than the DNS binaries for constraining gravity theories alternate to general relativity.

Finally, we note that the pulsars' zoo has been very recently enriched by a very intriguing object, PSR J0337+1715, which is a a *fully recycled* radio pulsar with

two white dwarf companions in a hierarchical triple system [38]. Besides raising new questions about its formation and evolution [39], it promises to be an excellent laboratory for studying the Strong Equivalence Principle, as it will be described in section 4.1.

3 Key-Notes on pulsar timing

When a new pulsar is discovered, the only known parameters are the approximate rotational period P and dispersion measure (DM)[1], as well as the very approximate position of the source in celestial coordinates. The possibility of an accurate determination of P, DM, and position in the sky, as well as the measurement of many other parameters of the targeted pulsar, results from undertaking a procedure dubbed *timing*. Although timing can be applied to any pulsar, the best results are obtained for those pulsars which behave as very stable rotators and whose flux density is large enough for an accurate determination of the "Times of Arrival" (ToAs) of the radio pulses. This is the case for some of the rapidly spinning recycled pulsars.

Excellent references for a thorough discussion on the pulsar timing procedures are represented e.g. by Chapters 7 and 8 of [40], as well as Chapters 4 and 5 of [41] (and Chapter 6 of [42] for an historical view).

3.1 First step: determination of the ToAs

On a practical ground, timing a pulsar means performing a campaign of semi-regular observations of the ToAs of some recognizable feature - e.g. the peak - in the radio light curve (the so-called pulse profile) of the source. The total duration of the campaign depends on the aims of the experiment and ranges from about 1 year up to decades, when the pulsar is part of a Pulsar Timing Array (PTA, see last section). As to the cadence of repetition of the observations, a dense coverage (up to few observations a day for pulsars in a binary system) is required at the beginning of the timing procedure. At later times it usually ranges from bi-weekly to bi-monthly observations.

The vast majority of radio pulsars are weak radio sources, with their single radio pulses being well below the typical noise resulting from the contribution of the sky and that of the detector system. In view of that, a timing observation typically results in an array of $N_{sub} \times N_{ch}$ integrated pulse profiles, related to N_{sub} subsequent intervals of the observation time (sub-integrations) and to N_{ch} frequency intervals (sub-bands), spanning the total available bandwidth. Each of these profiles is obtained by de-dispersing the signal within each sub-band using the best available value for the DM of the source and folding the data in each sub-band and each sub-integration at

[1] That represent the integrated column density of free electrons along the line of sight to the pulsar

a constant period, corresponding to the expected apparent spin period of the source. Each pulse profile is also carefully time-tagged, using an accurate clock which is installed at the radio observatory and is in turn regularly monitored and compared with the time distributed by the Global Positioning System (GPS).

Each of the pulse profiles is then compared with a very high signal-to-noise (S/N) standard profile, typically obtained from summing in phase a large number of observations of the given pulsar at the given frequency. This comparison produces a set of so-called *topocentric* ToAs, which are calculated by adding at the reference time of any pulse profile, the fraction of spin period by which the pulse profile is shifted with respect to the standard profile. Roughly speaking, the characteristic rms uncertainty in the determination of a topocentric ToA scales as the ratio between the width of the pulse in seconds and the signal-to-noise of the pulse profile.

3.2 Second step: modeling the ToAs

The aim is to use the pulses from a pulsar as the ticks of a clock, i.e. being able to count all the pulses arrived from a reference epoch $t_{\rm ep}$ to the present time t and to predict the times of arrival of all next pulses. With no loss of generality, we can assume that a pulse arrived exactly at $t_{\rm ep}$ and model the rotational evolution of the neutron star with a power series:

$$N(t) \;=\; \nu_{\rm ep} \times (t - t_{\rm ep}) + \frac{1}{2}\dot{\nu}_{\rm ep} \times (t - t_{\rm ep})^2 + \frac{1}{6}\ddot{\nu}_{\rm ep} \times (t - t_{\rm ep})^3 + ... \qquad (4)$$

where $\nu_{\rm ep}, \dot{\nu}_{\rm ep}, \ddot{\nu}_{\rm ep}, ...$ are the neutron star spin frequency and its first and second and higher-order derivatives at the reference epoch $t_{\rm ep}$, whereas $N(t)$ represents the number of rotations occurred from $t_{\rm ep}$ to t. The aim of the timing procedure is to determine $\nu_{\rm ep}, \dot{\nu}_{\rm ep}, \ddot{\nu}_{\rm ep}, ...$ with an accuracy high enough that $N(t_{\rm next})$ will be very close to be an integer, for any future time of occurrence $t_{\rm next}$ of a pulse. In this framework, it is useful to introduce the so-called *timing residuals*, given by $R(t_{\rm i}) = N(t_{\rm i}) - n(t_{\rm i})$, where $n(t_{\rm i})$ is the nearest integer to $N(t_{\rm i})$. We can state to have got a satisfactorily coherent timing solution for a pulsar over a time-span $\Delta t_{\rm span}$ if $R(t_{\rm i}) \ll 1$ for all the observed ToAs $t_{\rm i}$ in the time range from $t_{\rm ep}$ to $t_{\rm ep} + \Delta t_{\rm span}$.

Of course, $R(t_{\rm i}) = R(t_{\rm i}; \alpha_1, \alpha_2, ..., \alpha_m)$, where $\alpha_1, \alpha_2, ..., \alpha_m$ are the m parameters of the adopted timing model (i.e. $\nu_{\rm ep}, \dot{\nu}_{\rm ep}, \ddot{\nu}_{\rm ep}$ in the simple 3-parameter case discussed so far) and that naturally provides an operational way for improving a timing solution with a multi-parametric least squares fit, aimed to minimise the expression

$$\chi^2 \;=\; \Sigma_i \left(\frac{R(t_{\rm i}; \alpha_1, \alpha_2, ..., \alpha_m)}{\varepsilon_{\rm i}} \right)^2 \qquad (5)$$

where $\varepsilon_{\rm i}$ is the uncertainty on the i-th ToA in units of the pulsar spin period and i runs over all the available ToAs in the given time-span.

At the end of the day, one ideally expects to have a set of uncorrelated timing residuals, which should appear randomly scattered (i.e. with no evident trend) about a zero mean value when they are plotted versus the times of their collection t_i. A useful figure of merit for evaluating the quality of the timing solution is the ratio η between the root mean square (rms) of the residuals and the rotational rate of the pulsar, with $\eta \lesssim 0.001$ usually indicating a good solution.

What described above would be the whole story if the topocentric ToAs were collected in an inertial observing frame and when the neutron star had no binary companion. However, at least the first hypothesis is always wrong and the first step in the timing procedure is to convert the topocentric ToAs to the so-called *barycentric* ToAs. For each topocentric ToA t_i, this implies to calculate the corresponding Time of Arrival $t_{i,bary}$, as it were detected at the Solar System Barycenter (SSB, an acceptable approximation of an inertial frame) by a detector operating at an (in principle) infinite frequency. In a formal way, the conversion formula reads like:

$$t_{i,bary} = t_i + t_{\rm clock} - \frac{D}{f^2} + \Delta R_\odot + \Delta E_\odot + \Delta S_\odot \tag{6}$$

The value of $t_{\rm clock}$ results from the sum of various terms of correction (the so-called *clock correction chain*) and it is added retroactively, using tabulated values published by the *Bureau International des Poids et Mesures* (BIPM): the aim is to convert the time obtained at the telescope to the Terrestrial Time (TT) realization of the *Temps Atomique International (TAI)* [i.e. TT(TAI)], which differs (since 1971) from the TAI by a constant offset.

The next term in Equation 6 takes into account the effect of the dispersion of the radio pulses in the interstellar medium (see §1). In particular:

$$D(t_i) = \frac{e^2}{2\pi m_e c} \int_0^d n_e {\rm d}l = \mathscr{D} \times {\rm DM}(t_i) \tag{7}$$

where $\mathscr{D}$=$(4.148808 \pm 0.000003) \times 10^3$ MHz^2 pc^{-1}cm^3 s is the dispersion constant, d the distance to the pulsar, f is the Doppler-corrected observing frequency.

In general the fourth term in Equation 6 – also known as Roemer delay – gives the dominant contribution to the barycentric correction. It can be written as

$$\Delta R_\odot = \frac{\mathbf{r}\cdot\mathbf{n}}{c} + \frac{(\mathbf{r}\cdot\mathbf{n})^2 - |r|^2}{2cd} \tag{8}$$

where $\mathbf{n}$ is the unit vector on the line going from the SSB to the pulsar and $\mathbf{r}$ is the vector connecting the SSB and the Earth. Accounting for this term requires the knowledge of the location and motion of the major bodies in the Solar System and of the non-uniform Earth rotation. They are provided by the ephemeris published by the *Jet Propulsion Laboratory* [43] and by the bullettin regularly published by the *International Earth Rotation Service* [44].

Einstein's delay $\Delta E_\odot$ is a combination of the relativistic time delay and of the gravitational red-shift due, respectively, to the motion of the Earth and to the mass

of the other Solar System bodies. Its time derivative is given by:

$$\frac{d\Delta E_{\odot}}{dt} = \sum_k \frac{Gm_k}{c^2 d_{k,\oplus}} + \frac{v_{\oplus}^2}{2c^2} - \text{constant} \tag{9}$$

where G is the gravitational constant, m_k are the masses of the other Solar System bodies, $d_{k,\oplus}$ their distances to the Earth and $v_{\oplus}$ the velocity of the Earth with respect to the SSB.

Finally, the Shapiro delay $\Delta S_{\odot}$ [45] measures the extra time required for an electromagnetic wave to move in the curved gravitational field of a celestial body. In the framework of the pulsar timing, only the Sun and, sometimes, Jupiter, cause observable effects. In the case of the Sun, the formula takes the form:

$$\Delta S_{\odot} = -\frac{2GM_{\odot}}{c^3} \ln(1 + \cos\theta) \tag{10}$$

where θ is formed by the vector from the pulsar to the telescope with the vector from the telescope to the third body.

If the pulsar is included in a binary system, the *pulsarcentric* ToAs (i.e. the ToAs expressed in pulsar proper time at the pulsar surface) must also be corrected calculating them at the Pulsar Binary System Barycenter, before translating them to the Solar System Barycenter. This involves the introduction of 4 additional terms in the Equation 6:

$$t_{i,bary}^{Bin} = t_{i,bary} + \Delta R_{Bin} + \Delta E_{Bin} + \Delta S_{Bin} + \Delta A_{Bin} \tag{11}$$

Again, the Roemer term ΔR_{Bin} generates the largest effects: the ToAs anticipate when the pulsar is in front of the companion and are delayed when it is behind it. In a purely Newtonian framework, fitting for the orbital modulations of the ToAs allows one to derive five Keplerian parameters describing the binary system: namely, the orbital period P_b, the eccentricity e, the projection of the semi-major axis along the line of sight $x = a\sin i$, the longitude of the periastron ω (typically calculated with respect to the ascending node) and the epoch of the passage at the periastron T_0. Only in few favorable cases [46], the position angle on the sky of the ascending node (i.e. a sixth Keplerian parameter) can also be measured. From the Keplerian parameters one can derive the *mass function*:

$$f(M) = \frac{(M_c \sin i)^3}{(M_p + M_c)^2} = \frac{4\pi^2 (a\sin i)^3}{GP_b^2} \tag{12}$$

where M_p is the pulsar mass and M_c is the companion mass. Assuming a value for M_p and an edge-on orbit ($i = 90°$), it is possible to derive a lower limit for M_c.

The other terms in Equation 11 express the deviations from the predictions of the classical physics expected for a binary pulsar when it experiences strong gravitational fields and/or an high orbital velocity. These effects, and the related measurable parameters, will be explained in next section 4. It is worth noting that ΔA_{Bin} incor-

porates the effects of the changing aberration along the orbit and, strictly speaking, it is a classical physics effect. However, since the two related aberration parameters are almost degenerate with some post-Keplerian relativistic parameters (see later), this term is usually also described in the context of the relativistic effects.

In practice, one typically starts with a model having the minimum number of parameters, typically $\nu_{\rm ep}$ and the celestial coordinates of the pulsar. A poor determination of the pulsar spin frequency $\nu_{\rm ep}$ imprints a linear trend in the timing residuals plotted over the usually very short initial time-span. Instead, an error in the spin derivative imprints a parabolic trend in the residuals and the errors in the celestial coordinates leave a sinusoidal signature with a period of 1 year. If the pulsar is in a binary system, many additional trends in the residuals overlap with the ones mentioned above. *Solving* a pulsar means removing all these trends over a year long time-span. This is not only the result of a large series of trials and errors, but requires a good deal of experience, perseverance and educated feeling, as well as a touch of insight, in turn throwing a flash of artistic inspiration on the whole procedure.

We conclude this key notes on the timing procedure noticing that, unfortunately, not all the about 2000 radio emitting neutron stars are equally good time keepers: e.g. there are many sources exhibiting glitches (i.e. sudden increases in the spin frequency) and/or other timing irregularities. The former have been long thought to be related to some event occurring in the neutron star interior, although the exact origin of the process is still matter of debate (e.g. [47, 48, 49]). The timing noise has been only recently recognized to be most likely a phenomenon related with instabilities occurring in the magnetosphere of the pulsars [50]. Observations show that the two effects pertain mostly to the youngest and the ordinary pulsars, whose timing residuals display long term and unpredictable variations [51]. On the contrary they are virtually absent (or present at a very low level, e.g. [52]) in the population of the recycled pulsars, at least within the present level of precision in the measurements of the ToAs [53].

The considerations above indicate that the recycled pulsars are intrinsically better clocks than the bulk of the ordinary pulsars. Moreover the accuracy of the measurement of the ToAs roughly scales with the width of the pulses and hence, in turn, with the rotational rate. As a consequence, the fast spin rate of the recycled pulsars allows one to determine their ToAs with an higher accuracy than for the ordinary pulsars. However, at least three additional characteristics are very important in evaluating the quality and the potentialities of a recycled pulsar as a clock: the flux density, the shape of the pulse and the timing stability.

4 Pulsar tests of relativistic gravity

To first approximation, the amplitude of the deviations of general relativity with respect to Newtonian gravity can be evaluated by comparing the classical gravitational potential energy $E_{\rm gr} \sim -GM^2/R$ of a body of mass M and radius R with the rest mass energy of the same body, $E_{\rm rm} = Mc^2$ (c being the speed of light in vacuum and

G the gravitational constant). For the Earth the dimensionless ratio $\varepsilon = |E_{\rm gr}/E_{\rm rm}|$ is tiny ($\sim 10^{-10}$) and then most of the tests of general relativity have been carried on in space, involving various bodies of the Solar System (e.g. [54]). A detailed description of some of these experiments (the earliest of them, performed by Eddington on 1919, dates more than ninety years ago) is reported in the chapters by Iafolla, by Peron and by Turyshev in this book, whereas the chapter by Dell'Agnello mostly deals with future experiments of this class. All these experiments fully exploit a unique feature of general relativity, i.e. the absence of tunable parameters in the theory. As a consequence, even a single observation in disagreement with the predictions of the theory would unambiguously determine the falsification of the theory, at least in the physical regime of validity of the given observation. It is well known that to date general relativity passed *cum laude* all these potentially lethal tests (e.g. [55] for a recent review). However, even for the Sun ε is only $\sim 10^{-6}$, implying that all the experiments carried on in the Solar System can only explore the so-called *weak-field* limit of gravitational physics.

Despite the observational successes of general relativity, a wealth of alternate gravity theories kept on being proposed. Some of these theories have been already disproved by the observations, whereas many others preserve only a historical and/or academic relevance. However, few of them are still particularly interesting, since they emerged in the context of the studies aimed to build the long sought unified theory of the physical interactions, i.e. a theory capable to include electroweak and nuclear interactions in the same framework as the gravitational effects. Nowadays, a major obstacle in this direction is to match the probabilistic approach involved in the treatment of the first two phenomena with the deterministic predictions of general relativity. Following this reasoning, one may wonder whether other theories of gravity may lead to solve the dichotomy, while providing a better description of the behaviour of Nature in the extreme physical conditions of application of the putative unified theories, e.g. in the first fractions of second after the Big-Bang (some of these theories are described in depth elsewhere in this book, e.g. in the chapter by Diaferio & Angus, the one by Liberati & Mattingly as well as the chapter by Antoniadis).

The considerations above emphasize the need of performing tests of general relativity and/or of alternate gravity theories under the so called *strong-field* limit (corresponding to a value of ε close to unity), which is the regime associated to the notion of *extreme physical conditions* in presence of gravitational effects alone. In particular on one side it is very important the derive tight constraints to the falsifiability of general relativity in the strong-field regime, where the Einsteinian theory could finally reveal the existence of limits to its application. On another side, it has been shown [56] that there exist alternative theories which could pass all the tests in the weak-field limit, but would be violated as soon as the strong-field regime is approached; that makes the strong-field tests mandatory to properly test those theories.

In this context, two factors – described below – allow some binary recycled pulsars to become superb tools for investigating gravity theories. (I) It holds $\varepsilon \sim 0.2$ at the pulsar surface, which reflects the large gravitational binding energy (i.e. *self-*

field energy) of the neutron star. We here note that for all the known binary pulsar systems, the orbital separation is large with respect to the neutron star radius and so any binary component moves in the weak gravitational field of the companion. However, in most alternate theories of gravity (but not in general relativity), the orbital motion and the gravitational radiation damping depend on the *self-field energy* of the binary components. Therefore, when ε is large (i.e. of order unity), significant deviations – attributable to strong-field effects – are expected with respect to the orbital motion predicted by general relativity. (II) The radio signal behaves as an accurate and stable clock, which leads to accurately map the rotation and the orbit of the pulsar by means of the timing procedure described in §3. From the combination of the facts (I) and (II) it results the intriguing possibility of using some binary pulsars as unique laboratories for testing the strong-field regime of the gravity theories. In particular, the best binaries are those for which the properties expounded in (I) and (II) are particularly prominent.

General relativity and all the other in-principle-acceptable (i.e. with some chance to be *viable* [57]) alternate gravity theories can be grouped under the very large class of the so-calld *metric theories of gravity*. They satisfy the following three assumptions: *[a]* a symmetric metric exists; *[b]* all test bodies follow geodesics of the metric; *[c]* in local freely falling reference frames, all the *non*-gravitational laws of physics are those written in the language of special relativity. In other words, in all metric theories, gravitation must be a phenomenon related with the occurrence of a *curved space-time*. Although matter and *non*-gravitational fields respond only to the metric, additional fields can occur, giving rise to e.g. tensor/scalar theories, tensor/vectorial theories and so on... These additional fields prescribe how matter and *non*-gravitational fields contribute to create the metric; once determined, the metric alone acts back on the matter. Of course, at variance with the case of general relativity, these theories include a set of tunable parameters, associated to the additional fields. A detailed review of various gravity theories appeared e.g. in the textbook [54], which can be complemented with some recent updates [57, 55], as well as with the chapter by Will in this book.

4.1 Gravity theory tests using the PPN parameters

A first class of tests of metric theories of gravity involving pulsar observations is based on the parametrized post-Newtonian (PPN) formalism. In this framework, the deviations of any given theory from Newtonian physics are reflected in the values assumed by 10 parameters (the so-called PPN parameters, see e.g. [55] and the chapter by Will in this book), each of them connected with a given physical effect, such as the existence of preferred frames, the occurrence of preferred locations, the non-conservation of the momentum, the non-linearity in the superposition of gravitational effects, the amount of space curvature produced by a unit mass. On the theoretical point of view, this formalism allows one to easily interpret the physical implications of the various proposed alternative gravity theories in the weak-field

limit. At the same time, on the experimental point of view, the comparison between the observed and the predicted values of the PPN parameters provides an observational tool for directly constraining the falsifiability of general relativity and other theories. In effect, the PPN formalism was originally conceived (e.g. [58]) and then fruitfully used for performing a variety of tests in the weak-field environment of the Solar System [54, 57, 55]. Its extension to the case of the compact objects (i.e. including strong self-field effects) was elaborated in the Nineties [56] at least for a large class of tensor-multi-scalar gravitational theories [59]. That implied a partial redefinition of the 10 original PPN parameters, with the introduction of correction factors which are approximately dependent on the value of the dimensionless ratio ε introduced above. As a matter of fact, these factors can be safely neglected for the Solar System tests ($\varepsilon \lesssim 10^{-6}$), but not when dealing with neutron stars ($\varepsilon \sim 0.2$), which highlights again the fact that the pulsar tests of gravity are complementary to the tests involving bodies of the Solar System.

A detailed reading about pulsar experiments using the PPN formalism is given in the excellent online summary [60]. A particularly interesting case is that of the tests of the *Strong Equivalence Principle* (SEP). That is not only satisfied by general relativity, but it is conjectured to imply general relativity itself (e.g. [54]). It includes both the *Weak Equivalence Principle* (WEP) and the *Einstein Equivalence Principle* (EEP). WEP states that the trajectory of a free falling test body in a gravitational field is independent of its composition and internal structure (i.e. what is often referred to as the universality of free fall), whereas EEP adds that the outcome of any local non-gravitational experiment is independent (i) of when, (ii) of where in the universe and (iii) of the velocity of the freely falling reference frame in which it is performed (Lorentz and positional invariance of the non-gravitational laws of physics, see the chapter by Liberati & Mattingly in this book for details). SEP extends WEP to self-gravitating bodies (i.e. not only test bodies, but also bodies with a significant amount of internal gravitational energy, i.e. having a large value of the parameter ε) and EEP to experiments involving gravitational forces (like for instance the measurement of the position of the axes of the orbit followed by two bodies).

Therefore a simple test of the SEP is to check for the occurrence of differences in the trajectories of two massive bodies in a gravitational field. In particular Nordtvedt [61] first proposed to search for the occurrence of a "polarization" in the direction of the Sun of the orbit of the [Earth+Moon] system, caused by the different *self-field energy* of the two bodies (a phenomenon often called *Nordtvedt effect* or *gravitational Stark effect*). Using Lunar Laser Ranging (LLR) experiments it has been possible to set a strong limit to a linear combination of various PPN parameters in the typical conditions of the Solar System. In a similar way, the study of the "polarization" of the [pulsar+white dwarf] binaries in the Galactic gravitational potential allows one to set a limit to the violation of the SEP also in presence of strong self-field effects (in principle provided by the NS in the binary). At variance with the case of the [Earth+Moon] system, the geometrical and orbital parameters of a given [pulsar+white dwarf] binary are usually only partially known, which prevents the use of a single binary to perform the test. However, a statistical approach can be adopted: e.g. [62] used 21 [pulsar+white dwarf] binaries with long orbital periods

($P_b > 4$ days) and very low eccentricity ($10^{-6} \lesssim e \lesssim 10^{-3}$) in order to put a 95% confidence upper limit on Δ of 5.6×10^{-3}, where $\Delta = (M_{gr}/M_{in})_{\rm NS} - (M_{gr}/M_{in})_{\rm WD}$, with $(M_{gr}/M_{in})_i$ being the ratio between the gravitational and the inertial mass of the i-th body (of course, if SEP holds true, $(M_{gr}/M_{in})_i = 1$ for any i-th body and so $\Delta \equiv 0$). More recently, using a extended sample of 27 [pulsar+white dwarf] binaries, [63] improved the constraint to $\Delta < 4.6 \times 10^{-3}$. The possibility for a direct (vs the *statistical* approach presented above) determination of Δ relies on the measurement of the derivative of the eccentricity $\dot{e}$ in pulsar binaries [64]. Although the best limits from this approach [65] are not yet as constraining as those resulting from the statistical analyses above, the prospects are very promising, in view of the continuous improvement in the technology of the pulsar instrumentation and the availability of decades-long data spans [65].

Besides the aforementioned *gravitational Stark effect*, many other phenomena related to violations of the SEP manifest as *polarization* of the orbit or as *precession* of the orbit or of the spin axis of the neutron star, as well as the occurrence of an additional acceleration applied to the neutron star or to the centre of mass of the binary, Accurate pulsar timing of one binary (or of an ensemble of suitable binaries) can unveil and measure those effects, thus putting constraints to various PPN parameters. These limits are often much better than those obtained in the Solar System: an illustrative case is that of the parameter $\hat{\alpha}_3$ (where $\hat{\alpha}_i$ denotes the strong-field generalization of the PPN parameter α_i). A non-zero value of $\hat{\alpha}_3$ would imply the occurrence of preferred reference frames, as well as the non-conservation of the momentum. By using the data from an ensemble of [pulsar+white dwarf] binaries one can get a limit $\hat{\alpha}_3 < 4 \times 10^{-20}$ [62] (95% confidence level), which is 13 orders of magnitude better than that derived from the measurements of the perihelion shift of the Earth and of Mercury [54]. Similarly, strong-field limits on the other two PPN parameters ($\hat{\alpha}_1 = -0.4^{+3.7}_{-3.1} \times 10^{-5}$ [66] and $|\hat{\alpha}_2| < 1.6 \times 10^{-9}$ [67], 95% confidence level) which involve, like $\hat{\alpha}_3$, the existence of preferred frame effects (i.e. a violation of the Lorentz invariance) have been obtained from the timing analysis of the binary pulsar PSR J1738+0333 [36, 37] (in this case the limit is about one order of magnitude better that than derived for α_1 from Lunar Laser ranging experiments [68]), as well as exploiting the observations of two isolated millisecond pulsars, PSRs B1937+21 and J1744−1134 (in this case the constraint is two orders of magnitude stronger that than obtained for $|\alpha_2|$ with the best test performed in a weak field, i.e. the alignment of the Sun spin with the total angular momentum of the Solar system [69]). It is worth noting that the current best limit on $|\hat{\alpha}_2|$ is not obtained from the study of binary pulsars, but it results from the analysis of the secular stability of the pulse profile of the two aforementioned solitary pulsars. In fact, a non-vanishingly small $\hat{\alpha}_2$ would induce the precession of a pulsar spin (and hence a secular variation in the observed pulse profile) around the pulsar direction of motion with respect to the putative preferred frame. An analogous precessional effect leads to the possibility of using the same pulse profile data of the two millisecond pulsars above for deriving the strongest available limit on the parameter $|\hat{\xi}| < 3.9 \times 10^{-9}$ (95% confidence level) [70] (the strong-field counterpart of the Whitehead PPN parameter ξ), that turns out to be six orders of magnitude more constraining than the

previous best limit on ξ obtained in the weak gravitational field environment of the superconducting gravimeter experiments [71].

On other cases, the pulsar timing tests are nominally less constraining than the Solar System tests; however – as explained above – they explore a different regime of gravity with respect to the Solar System tests. For example, an upper limit $\zeta_2 < 4\times10^{-5}$ to the non-conservation of the momentum (embodied in the PPN parameter ζ_2) also resulted from the analysis of PSR B1913+16 [72]. Furthermore we note that the occurrence of preferred positions and times in the universe may naturally lead to variations in the fundamental constants, like e.g. the gravitational constant *G*. Pulsar timing can put constraints also on this effect, as described in section 4.2.3, when dealing with the case of the binary pulsar PSR J0437−4715. Interestingly, the limit on $|\hat{\xi}|$ can also be converted into an upper limit of 4×10^{-16} on the spatial anisotropy of the gravitational constant [70].

Additional relevant improvements in constraining the SEP are expected from the timing of the first known millisecond pulsar (PSR J0337+1715) in a hierarchical triple system with two other compact stars, both white dwarfs, a recently announced (Jan 2014) milestone discovery [38] in pulsar science. The classical newtonian effects occurring in this 3-body system (complemented with the inclusion in the model of the special-relativistic transverse Doppler effect) have already led to a precise determination of the masses of the pulsar ($1.4378\pm0.0013\,M_\odot$) and of the two companions ($0.19751\pm0.00015\,M_\odot$ and $0.4101\pm0.0003\,M_\odot$), as well as to a measurement of the inclinations of the orbits, surprisingly almost co-planar (close to ~ 39.2 deg [38]). The pulsar and the inner white dwarf (orbiting the common center of mass in about 1.6 days) are two bodies having a very different self-field energy ($\varepsilon\sim0.2$ for the neutron star, whereas $\varepsilon\sim10^{-4}$ for the white dwarf, see section 4 and section 4.2.3) and both moving in the gravitational field provided by the outer white dwarf (having an orbital period of about 327 days). Since the latter field is 6-7 orders of magnitude larger than the gravitational field due to the Galaxy, any putative SEP violation occurring in the J0337+1715 inner binary would be strongly magnified with respect to the case of all the previously described [pulsar+white dwarf] binaries, thus making the new triple system the best laboratory for investigating the limits of the SEP.

4.2 Gravity Theory tests using the PK parameters

When a pulsar is orbiting another compact object (a second neutron star or a white dwarf) in a close enough orbit, the very high orbital velocity and the large deformation of the space-time produced by the two massive stars in the system can lead to stronger relativistic effects than those described in § 4.1. This may open the possibility of directly measuring these effects on the times of arrival of the pulses from the pulsar(s) and, in turn, to carry on a direct comparison between the observations and the predictions of the various theories of gravity.

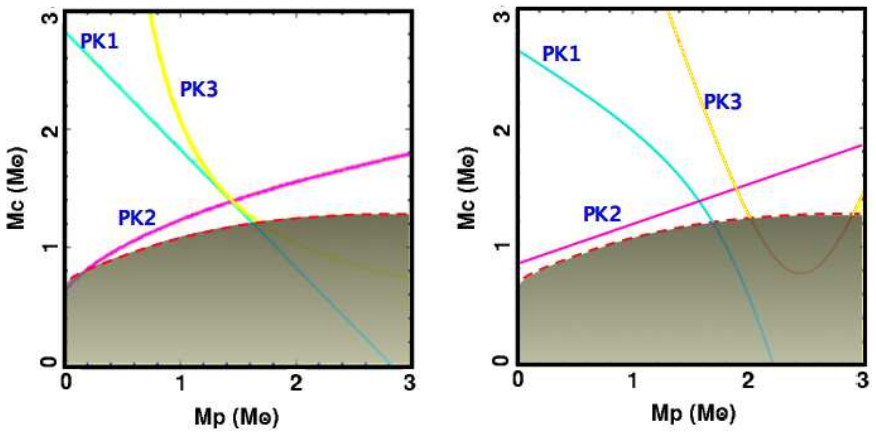

Fig. 3 Mass-vs-mass diagrams of a binary system for which three post-Keplerian parameters have been measured. The two panels refers to two alternate gravity theories. Each color-coded curve in the panels describes the constraint on the masses of the two orbiting bodies resulting from the same observed value of a given PK parameter (and its uncertainty), combined with the adoption of the gravity theory specific to that panel. *Left panel*: Since a common area exists for the three curves, this gravity theory survives the test. *Right panel:* No overlap exists for the three curves, implying the rejection of this gravitational theory.

In this context, Damour and Deruelle [73, 74] developed a powerful and successful framework, tailored for constraining a very large class of gravitational theories. It relies on the introduction of the so-called *post-Keplerian* (PK) parameters, which satisfy the following two very useful properties: *(i)* the PK parameters are phenomenological quantities, which can be measured according to a well established operational prescription, independent on the adopted gravity theory; *(ii)* in any specific gravity theory (chosen in a large range of metric theories), the PK parameters can be written as function of the pulsar and companion masses and of the Keplerian parameters of the binary system.

Since the Keplerian parameters are easily determined with a precision much better than any PK parameter, they can be regarded as well known terms in the formulae for the PK parameters, which leaves only two unknown quantities (the pulsar and companion masses) in each formula. As a consequence, the measurement of two PK parameters results in the determination of the masses of the two stars in the system, the values of which are expected to depend on the adopted theory of gravity. On the other hand, the measurement of $N_{\rm PK} > 2$ PK parameters yields $N_{\rm PK} - 2$ independent self-consistency tests for the given theory. The methodology can be illustrated in a simpler way in the mass-vs-mass plot for the two binary components, where each PK parameter (with its uncertainty) is associated to a pair of lines (see Fig. 3). The region in the plot located between a pair of lines is the only allowed by the theory under investigation. If an area of overlap between the various pairs of lines exists, that specific gravity theory passes the test (see left panel of Fig. 3). Otherwise (e.g. right panel of Fig. 3) the theory has to be unequivocally rejected.

In the specific case of general relativity, the equations describing the 5 most used PK parameters assume the form [74, 75, 76]:

$$\dot{\omega} = 3\left(\frac{P_b}{2\pi}\right)^{-5/3}(T_\odot M)^{2/3}(1-e^2)^{-1} \tag{13}$$

$$\gamma = e\left(\frac{P_b}{2\pi}\right)^{1/3} T_\odot^{2/3} M^{-4/3} m_2 (m_1 + 2m_2) \tag{14}$$

$$\dot{P}_b = -\frac{192\pi}{5}\left(\frac{P_b}{2\pi T_\odot}\right)^{-5/3}\left(1+\frac{73}{24}e^2+\frac{37}{96}e^4\right)(1-e^2)^{-7/2}\frac{m_1 m_2}{M^{1/3}} \tag{15}$$

$$r = T_\odot m_2 \tag{16}$$

$$s = x\left(\frac{P_b}{2\pi}\right)^{-2/3} T_\odot^{-1/3} M^{2/3} m_2^{-1} \equiv \sin i \tag{17}$$

where m_1 and m_2 are the two star masses, $M = m_1 + m_2$, $x = a\sin i$ and $T_\odot \equiv GM_\odot/c^3 = 4.925490947\,\mu$s. The PK parameter $\dot{\omega}$ is phenomenologically associated with the advance of the periastron, γ is a parameter accounting for gravitational redshift and time dilation, $\dot{P}_b$ is the orbital damping and, in the framework of general relativity, measures the rate at which the orbital period decreases due to emission of gravitational radiation. Finally, r and $s \equiv \sin i$ represent respectively the *rate* and the *shape* of the so-called Shapiro delay [45], a time delay of the radio signal caused by the space-time deformations around the companion star. As expected, no tunable parameter appears in the set of equations above, whereas one or more theory dependent tunable parameters are contained in the arrays of equations resulting from adopting alternate gravity theories (see e.g. [54, 57] for a few examples).

4.2.1 The case of the Double Neutron Star binaries

The first very famous case of application of this class of tests is represented by the binary pulsar system B1913+16, discovered at Arecibo in 1974 [77]. It is a double neutron star system whose pulsar is rotating with a 59-ms period while completing a highly eccentric ($e = 0.61$) orbit in about 7.8 hr. Three PK parameters have been measured for this system: from equations 13 and 14, for $\dot{\omega}$ and γ respectively, the most precise values ever for the masses of two pulsars have been determined [78], and an accurate prediction for $\dot{P}_b^{\rm GR}$ resulted from inserting these masses in equation 15. It turned out that the observed intrinsic value $\dot{P}_b^{\rm int}$ (see later) for the rate of the orbital damping matched spectacularly with $\dot{P}_b^{\rm GR}$ (the agreement, after more than 3 decades of timing observations, is now at 0.2% level [78]). On one hand, that provided a spectacular proof of the occurrence of quadrupolar gravitational waves emission from the system, while, on another hand, that also showed that the internal structure (i.e. the *self-gravity*) of the neutron stars does not affect – at least not at more than the 0.2% level – the dynamics of the system, which can be described as it were composed by two point masses. This supports the so-called *effacement* of the

interior of the bodies [79], which is a property peculiar to general relativity (in turn arising from the Strong Equivalence Principle), while not holding in other gravity theories.

It is here important to note that $\dot{P}_b^{\rm int}$ is not directly the value $\dot{P}_b^{\rm ToA}$ resulting from the fitting of the observed ToAs to the timing formula, but it was corrected for various effects which can contaminate $\dot{P}_b^{\rm ToA}$. In fact in general it holds

$$\left(\frac{\dot{P}_b}{P_b}\right)^{\rm ToA} = \left(\frac{\dot{P}_b}{P_b}\right)^{\rm int} + \left(\frac{\dot{P}_b}{P_b}\right)^{\rm z} + \left(\frac{\dot{P}_b}{P_b}\right)^{\rm rot} + \left(\frac{\dot{P}_b}{P_b}\right)^{\rm Shk} + \left(\frac{\dot{P}_b}{P_b}\right)^{\rm other} \qquad (18)$$

where $\dot{P}_b^{\rm int}$ is the intrinsic rate of the orbital decay, while $\dot{P}_b^{\rm z}$ is the contribution to the apparent orbital damping due to the vertical acceleration in the Galactic potential [80] , $\dot{P}_b^{\rm rot}$ is the contribution due to differential rotation in the plane of the Galaxy [80], $(\dot{P}_b/P_b)^{\rm Shk} = [v_\perp^2/(cd)]$ (with d the distance and $v_\perp$ the transverse velocity of the binary system with respect to the SSB) is the Shklovskii effect, arising from the transverse component of the relative velocity of the binary barycenter with respect to the SSB. Finally, $\dot{P}_b^{\rm other}$ summarizes other contributions which have been thoroughly investigated in [80] and which, in most cases, are negligible with respect to the other terms. A relevant exception is for the binary pulsars harbored in a globular cluster, whose gravitational potential well can impart a significant line-of-sight acceleration to the pulsar; in this case $\dot{P}_b^{\rm other}$ can overcome all the other contributions[2]. In the case of PSR B1913+16, the imperfect knowledge of the shape of the Galactic potential, and in turn of $\dot{P}_b^{\rm z}$ and $\dot{P}_b^{\rm rot}$, emerges now as the limiting factor acting against further large improvements of the accuracy of the test of general relativity.

The impact of the Galactic potential in the orbital period derivative is even more evident for the case of the 38-ms pulsar PSR B1534+12, discovered at Arecibo on 1990 [81] and also hosted in a double neutron star binary. All the 5 PK parameters listed in the equations 13→17 have been measured. The 3 PK parameters $\dot{\omega}$, γ, and s provided the first accurate test (at better than 1% level) for the non-radiative prediction of general relativity [82] and the range r of the Shapiro delay is also fully compatible with what expected from general relativity. However, the observed value $\dot{P}_b^{\rm ToA}$ is not compatible (at 1σ level) with the expectations of general relativity. This is interpreted as due to the large uncertainty on the correction to $\dot{P}_b^{\rm ToA}$ resulting from the Shklovskii contribution $(\dot{P}_b/P_b)^{\rm Shk} = [v_\perp^2/(cd)]$, in turn arising from the uncertain determination of the pulsar distance d. Assuming that general relativity is correct, one can invert the line of reasoning, obtaining a precise determination of the distance of the binary, which should be located at $d_{\rm GR} = 1.02 \pm 0.05$ pc. This is about a factor 30% farther away with respect to the distance inferred from the DM of the pulsar $d_{\rm DM} \sim 0.7$ kpc, in agreement with the typical uncertainty on the pulsar distances inferred from the value of their dispersion measure.

[2] This is likely the case for for the double neutron star system J2129+1210C [35] associated with the globular cluster M15

4.2.2 The unique case of the Double Pulsar

The second and unique other binary for which 5 PK parameters have been determined is the spectacular J0737−3039 system, also known as Double Pulsar. In April 2003 the discovery at Parkes of this unprecedented system [22, 23] represented a breakthrough in the science of the compact objects and started a new era in the study of relativistic gravity. The discovery occurred during a search for pulsars at High Galactic latitude (the so-called *PH-survey* [83]) performed at 1.4 GHz using the multi-beam receiver of the Parkes radio telescope. The discovery plot clearly manifested the occurrence of a strong line-of-sight acceleration (about 100 m s^{-2}) on the pulsar, indicating that it was experiencing a relevant gravitational pull from a massive companion.

Three subsequent $\sim$ 5-hr long integrations provided the radial velocity curve suggesting that it was a double-neutron-star binary system with an orbital period of only 2.4 hours and an eccentricity $e \sim 0.09$. Subsequent observations also showed that both the compact objects were observable as a radio pulsar: PSR J0737−3039A (hereafter labelled as psrA) is a mildly recycled pulsar with a rotational period of about 22 ms, whereas PSR J0737−3039B (hereafter dubbed psrB) is an ordinary pulsar with a spin period of about 2.7 s.

At least four features conjure in order to make this binary an unprecedented laboratory for studying general relativity: *(a)* the large velocity of the stars along their orbit (more than 300 km s^{-1}, i.e. about one thousandth of the speed of light in the vacuum); *(b)* the small distance between the two stars (between about 2 and 3 times the Earth-Moon distance); *(c)* the high orbital inclination (above 88°); *(d)* the observability of the radio pulses from both the stars, allowing one to use them as two *clocks* in the binary. In particular, the first two factors lead to significant relativistic effects, while the features *(c)* and *(d)* simplify the detectability of the effects with the timing procedure.

As a result, only few timing observations (spanning no more than about one week) were enough to measure the relativistic advance of periastron $\dot{\omega}$ of psrA [22]: about 16.9° yr^{-1}, significantly larger than ever observed before. Six months of additional ToAs led to determine three further PK parameters, i.e. the combined time dilation and gravitational red-shift parameter γ, as well as the range r and the shape s of the Shapiro delay. The observability of both the pulsars made also possible to independently determine the size of the two orbits, which in turn – using the Kepler third law – led to the first direct measurement of the mass ratio R [23] in a double neutron star system. It is worth noting that the value of R is not affected by the *self-field* effects (at least for a very large class of metric theories of gravity), in contrast with the PK parameters [74]. In terms of the mass-vs-mass plot, that implies that the location of the pair of straight lines – both passing from the origin of the plot – which are associated with R (and with the observational uncertainty on R) is independent of the specific gravity theory.

The fifth PK parameter (i.e. the orbital decay $\dot{P}_b$) was also detected with high significance after another year of data taking. That confirmed that the system shrinks at the pace of about 7 mm day^{-1} and it will end up into a merging of the two neu-

tron stars in ~ 85 million years, owing to emission of gravitational waves. This fact, combined with the short distance of this system, makes the Double Pulsar the dominant binary in the calculations for the merger rate of double-neutron-star systems in our Galaxy and in the rest of the Universe [22]. Despite the many uncertainties still affecting the prediction of the absolute rate for those events, the discovery of the Double Pulsar determined a significant relative increase (up to about an order of magnitude, e.g. [84]) in any model, triggering new hopes for the ongoing ground-based interferometric experiments (e.g. LIGO and VIRGO) aimed at the detection of gravitational waves.

An additional relativistic effect – the *relativistic precession* of the spin axis of psrB[3] – has been more recently measured in the Double Pulsar system, exploiting the occurrence of short eclipses (~ 30 s long) of the radio signal from psrA (at least at frequencies smaller than ~ 1.4 GHz) when it transits at the superior conjunction. Four years of observations revealed a clear linear evolution in the azimuthal spin axis angle, that is the angle which describes the precessional motion of the spin vector of psrB around the total angular momentum vector. The measured rate $\Omega_B = (4.77^{+0.66}_{-0.65})^\circ$ yr^{-1} [86] is compatible, at the 13% level, with the prediction of general relativity [87], $\Omega_B^{\rm GR} = (5.0734 \pm 0.0007)^\circ$ yr^{-1}.

Although this effect has been somehow observed in other binary pulsars (e.g. see [88] for PSR B1534+12 and [89, 90, 91] for PSR B1913+16, and more recently see [92] for PSR J1141−6545), only in the case of the Double Pulsar it provides a significant test both to general relativity and to alternate gravity theories. In fact, when dealing with the class of the Lorentz-invariant gravity theories based on a Lagrangian [76] – general relativity of course belongs to that class – one can write the following general formula for the relativistic spin precession rate of the neutron star labelled as B in the system:

$$\Omega_B = \left[\frac{x_A x_B}{s^2}\right]\left[\frac{8\pi^3}{(1-e^2)P_b^3}\right]\left[\frac{c^2\sigma_B}{G_{AB}}\right] \tag{19}$$

where x_A, x_B are the projected semi-major axes of the orbits of the two neutron stars in the system, σ_B is a (theory dependent) *strong-field spin-orbit* coupling constant and G_{AB} is the gravitational constant – also theory dependent! – for the gravity interaction between the two pulsars, whereas the other quantities are the usual Keplerian and PK parameters and constants as defined in previous sections. In order to solve for the rightmost factor one needs a measurement of the spin precession, a precise determination of s, and, separately, of x_A and x_B, which means that the binary must satisfy at least the three following properties: *(i)* a high spin precession rate, *(ii)* a highly inclined orbital plane and *(iii)* the observability of both the neutron stars as pulsars. These features simultaneously hold only for the fortunate and so far unique case of the Double Pulsar, for which, inserting the measured parameters in equation 19, one obtains $\left[\frac{c^2\sigma_B}{G_{AB}}\right] = 3.38^{+0.49}_{-0.46}$. This provides an unprecedented strong-field

[3] In many papers related with pulsars, this effect is referred to as *geodetic* (or as *De Sitter*) *precession*. For a brief description of the apparently discrepant terminology see e.g. [85].

test for all the gravity theories belonging to the large aforementioned class: a theory can survive only if it predicts for $\left[\frac{c^2\sigma_B}{G_{AB}}\right]$ a value in agreement with the one above. General relativity passes also this test, since in this theory $\left[\frac{c^2\sigma_B}{G_{AB}}\right]_{GR} = 2 + \frac{3m_A}{2m_B}$, and from the measured value of R, it results $\frac{3m_A}{2m_B} + 2 = 3.60677 \pm 0.00035$. As it involves the *strong self-field* of a neutron star, this test of general relativity has a wider nature with respect to the tests of the relativistic spin precession which have been performed and/or are in progress in the weak-field regime of the Solar System. In particular, it supports the extension to the rotating bodies of the already introduced concept of *effacement* of gravity in general relativity [79], which had been previously tested for the orbital motion only. Namely the internal structure of the neutron star does not prevent the star to behave like a spinning test particle in a weak external field[4].

With the measurement of the spin precession rate of psrB – implying the occurrence of a related pair of lines, labelled as Ω_B, in the mass-vs-mass diagram of the binary – there are now seven relativistic constraints (i.e. seven pairs of lines in Figure 4), for the values of the masses of the two neutron stars in the J0737−3039 system: five from the PK parameters, one from the mass-ratio R, and one arising from Ω_B. On top of those, there are the additional classical constraints derived from the Newtonian mass function of the pulsars. Inspecting the inset in Figure 4, one can see the existence of a common, although tiny, region of overlap for all the pairs of lines. As a consequence, after less than a decade from the discovery of the system, the observations of the Double Pulsar binary are already providing $7 - 2 = 5$ successful tests of self-consistency of general relativity in presence of strong-field effects [95]. The most stringent published test to date – and the best so far among all the gravitational experiments involving *strong-field* effects – is for the shape s of the Shapiro delay, which matches with the observations at 0.05% level [96].

Since there is still a large room for future improvement of the timing solution for the Double Pulsar[5], a wealth of further intriguing results are expected to flood from keeping on observing this system and from the introduction of more sensitive observational apparatuses. E.g. a recent interferometric determination of the parallax of the system [98] indicated that over a decade, $\dot{P}_b$ may be observed with an accuracy of $\gtrsim 0.01\%$, paving the way to stringent tests of the theories that predict dipolar gravitational radiation (contrary to the quadrupolar only contribution resulting from general relativity, see $ 4.2.3).

Continuous accumulation of ToAs will also lead to measure new PK parameters (such as the aberration ones), and to derive constraints on the existence of a preferred frame and thus on the violation of the local Lorentz invariance of gravity in the strong internal fields of the neutron stars [99]. Moreover, the availability of a (decennial) series of high quality ToAs may lead to unveil the signature of the second

[4] Note that, contrary to common expectations, no precession of the spin axis of psrA in the Double Pulsar has been detected so far [93], which may suggest the occurrence of a small misalignment angle between the orbital angular momentum and the spin axis of psrA, likely less than $\sim 15^\circ$ [94].

[5] The recent (but supposedly temporary) disappearance of the radio signal from psrB [97] will not hamper the improvement of the timing accuracy of the solution for psrA.

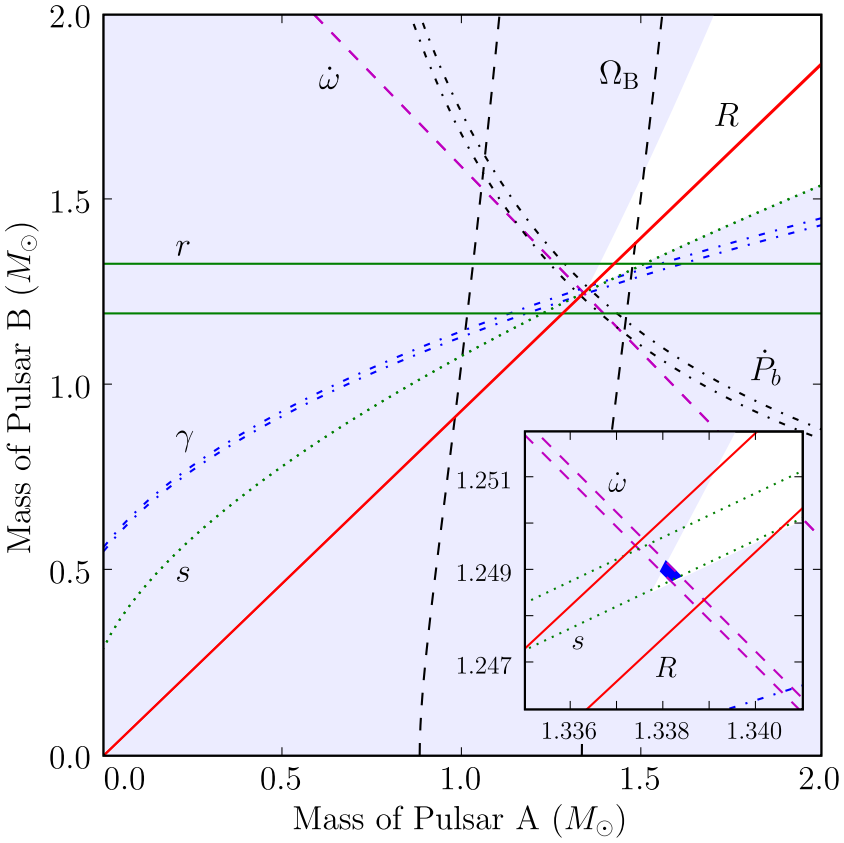

Fig. 4 Mass-vs-Mass diagram for the Double Pulsar system J0737−3039. The shaded regions are those that are excluded by the Newtonian mass functions of the two pulsars. Further constraints are shown as pairs of lines enclosing permitted regions as predicted by general relativity and related to the observation of the mass ratio R, the PK parameters and the precession rate Ω_B of the spin axis of psrB. Inset is an enlarged view of the small quadrilateral encompassing the intersection of all these constraints. (Courtesy of René Breton 2009).

order post-Newtonian corrections to the orbital periastron advance $\dot{\omega}$ of the system. This would be of paramount importance, since these corrections will include the value of the spin angular momentum of psrA, opening the intriguing perspective to measure that and therefore to determine the moment of inertia of psrA [100]. As a matter of fact, this measurement may finally reveal to be at the borderline of the possibilities of the current instrumentation [7], but might be attained when new more powerful radio-telescopes will enter in play. The scientific pay-back from that would be enormous, since the simultaneous determination of the mass and the moment of inertia of a neutron star would significantly constrain the equation of state for the nuclear matter [101], shedding light on a long standing and still unanswered fundamental question of the nuclear physics.

4.2.3 Other interesting cases and constraints on tensor-scalar theories

As discussed in previous sections there are few binary pulsars with a white dwarf companion for which one or more PK parameters have been measured. In most cases, they are only the shape *s* and range *r* of the Shapiro delay, which allow one to infer with good accuracy the mass of the companion, but are not enough for constraining the gravitational theories.

However, at the time of writing these notes there are at least four notable exceptions, the binary pulsars PSR J0437−4715, PSR J1141−6545, PSR J1738+0333, and PSR J0348+0432 (sorted in chronological order of discovery), the cases of which we briefly illustrate here, since their continuous timing is producing results which are complementary to those of the Double Pulsar and the other two relativistic double neutron stars (PSR B1913+16 and PSR B1534+12) which we previously described.

The former was discovered in 1993 during a survey at 400 MHz at the Parkes radio telescope [102]. Two factors make PSR J0437−4715 a primary target for high precision timing: its proximity to the Earth (it is indeed the closest known recycled pulsar, $d = 156.3 \pm 1.3$ pc [103]) and its brightness (flux density of 142 mJy at 1.4 GHz, a factor ~ 14 larger than the second most luminous recycled pulsar). In fact, the closeness to us produce significant geometrical effects, such us *(i)* the so-called *annual-orbital parallax* [104] (i.e. the apparent variation of the inclination angle of the binary system) due to the orbital motion of our planet and *(ii)* the apparent secular change in the projected semi-major axis of the pulsar orbit due to the pulsar proper motion [105]. Accounting in the timing model for these two apparent phenomena, and exploiting the exceptionally accurate ToAs achievable for this system, it was possible [106] to infer both the inclination angle *i* and the longitude of the ascending node (a Keplerian parameter which is usually not measurable via pulsar timing) of the system. The derived value of *i* – thus determined in a completely independent way – was then compared with the expected effects on the ToAs of the Shapiro delay, finding a nice agreement of the data with the prediction of general relativity, for which the PK parameter *s* is simply equal to $\sin i$. The best pulsar test on the time variation of the Newtonian constant of gravity *G* is also so far provided by this system: $|\dot{G}/G| < 23 \times 10^{-12}$ yr^{-1} (see [107]).

PSR J1141−6545 (discovered on 1999 at Parkes [108]) is a rare example of a binary pulsar, the white dwarf companion[6] of which is older than the neutron star, due to a reversal in the mass ranking of the two stars in the system – i.e. the originally less massive object became the most massive one after the first stages of mass transfer during the binary evolution [110]. Whence, the originally more massive star ended its evolution as a massive (1.02 ± 0.01 M$_\odot$) white dwarf [111], whereas the originally less massive star later exploded as a supernova leaving a relatively young (~ 1.4 Myr [108]) and not recycled (spin period of 394 ms) pulsar with a mass of 1.27 ± 0.01 M$_\odot$ [111], which is now orbiting the white dwarf in an elliptical and short orbit ($e \sim 0.17$, $P_b \sim 4.74$ hr) [108]. Despite the relatively

[6] The recent optical detection of the companion supports its being a white dwarf [109]

long rotational period, the latter two properties (as well as the brightness of the source) led to clearly detect three PK parameters (namely $\dot{\omega}$, γ, $\dot{P}_b$), allowing [111] to infer the masses of the two bodies (as reported above) and – after correction for the spurious effects of equation 18 – to test the radiative prediction (i.e. the damping of the orbit due to gravitational waves emission) of general relativity at better than 10% level [111]. Also, it has been very recently detected the occurrence of the *relativistic precession* [92] of the spin axis of the pulsar.

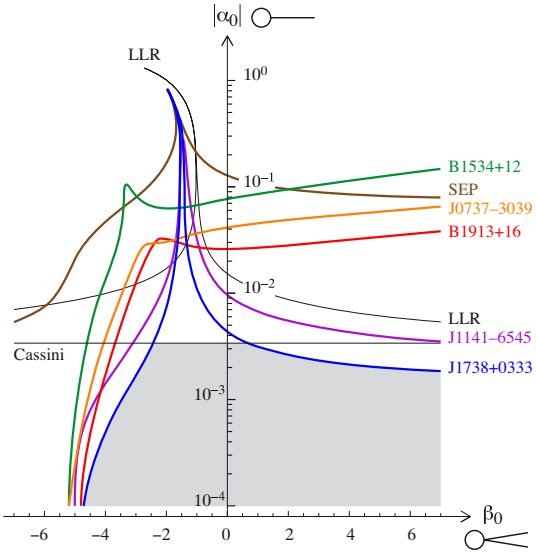

Fig. 5 Experimental contraints on the $|\alpha_0|$ (logarithmic scale) and β_0 (linear scale) constants of the coupling function $a(\psi) = \alpha_0\psi + 0.5\beta_0\psi^2$ of the matter with a scalar field ψ. The point in the diagram at coordinates ($|\alpha_0| \to 0$; $\beta_0 = 0$) corresponds to general relativity. The vertical axis corresponds to Brans-Dicke theory, whereas the horizontal axis is the locus of the theories which are indistinguishable from general relativity in the weak-field conditions of the Solar System experiments. The allowed regions are below the various solid lines, related to the observations of various binary pulsar systems (B1534+12, J0737−3039, B1913+16, J1141−6545, J1738+0333) and to the outcomes of several experiments performed in the weak-field limit of the Solar System, including the Lunar Laser Ranging (LLR) and the Cassini spacecraft's results. The shaded area is the one allowed so far by all the tests. It is evident the primary role of PSR J1738+0333 in setting some of the current limits (courtesy of Paulo Freire 2012 [37]).

Although the aforementioned test of general relativity with PSR J1141−6545 is far from approaching the accuracy of those obtained with the J0737−3039 or the B1913+16 systems, it is more useful than the other tests in constraining a particularly important class of alternate gravity theories, i.e. the so-called *tensor-scalar* theories, in which the usual tensor field is complemented with one scalar field ψ. Besides many other additional advantages (see e.g. [59, 112]), these gravity theories are a natural outcome of many unified theories (i.e. superstring, Kaluza-Klein, etc. [59, 112]) invoking a scalar counterpart for the graviton and they often appear as a key ingredient in cosmology for explaining the past or the current phases

of accelerated expansion (i.e. inflation, quintessence) of the universe. In particular, the *tensor-mono-scalar* theories can be grouped in a family, parametrized by two constants, α_0 and β_0, which describe the linear and the quadratic coupling between the matter and the additional scalar field, according to the expression $a(\psi) = \alpha_0\psi + 0.5\beta_0\psi^2$, where $a(\psi)$ is the coupling function, and $\exp[2a(\psi)]g_{\mu\nu}$ replaces the role of the ordinary spin-2 metric tensor $g_{\mu\nu}$ of general relativity. Of course, the Einsteinian theory is fully recovered for $\alpha_0 = \beta_0 = 0$, whereas e.g. the Jordan-Fierz-Brans-Dicke gravitational theory [113] is accounted for by assuming $\beta_0 = 0$ and $\alpha_0^2 = 1/(2\omega_{BD} + 3)$, where ω_{BD} is the Brans-Dicke parameter (e.g. [114]). In this context, the experimental tests aim to put constraints in the 2-dimensional space of (α_0, β_0), where the origin coincides with the theory of general relativity, the vertical axis with the Brans-Dicke theory, and so on [115]: one such plot is reported in Figure 5.

The orbital damping rate $\dot{P}_b$ is the most affected PK parameter by the occurrence of a scalar field. In particular the value of $\dot{P}_b$ should be enhanced by the emission of *dipolar* gravitational radiation (due to emission of scalar spin-0 waves) with a power of order $\mathcal{O}(1/c^3)$, superimposed to the quadrupolar component (associated to spin-2 gravitons) of general relativity having a much smaller power of order $\mathcal{O}(1/c^5)$. However, for two perfectly identical neutron stars in a binary, the dipolar term obviously vanishes and it almost cancels out also for two neutron stars of similar masses, since their compactness parameters (related to the dimensionless ratio ε) are supposed to be similar. This is not the case for a white dwarf, whose compactness parameter (and hence the coupling of matter with the scalar field) is expected to be much smaller than for a neutron star. Therefore the binary pulsars orbiting a white dwarf in clean binary systems (i.e. with no uncontrolled effects affecting $\dot{P}_b$, like tidal interactions or mass loss or magnetic braking...) are primary targets for investigating the occurrence of scalar waves and in turn for constraining the space of the parameters of the *tensor-scalar* theories.

Figure 5 illustrates the important role played by PSR J1141−6545 in this framework. However, another binary pulsar, PSR J1738+0333 (discovered during 2001 at Parkes [116] and orbiting a low mass white dwarf companion of ~ 0.18 $M_\odot$ in a ~ 8.5 hr orbit of low eccentricity, $e \sim 3 \times 10^{-7}$), recently gained the pole-position in the ranking of the most useful binary pulsars in testing (and constraining the parameters of) the tensor-scalar theories [37]. A decade-long timing campaign at Arecibo provided a determination of $\dot{P}_b$, as well as an extremely accurate determination of the proper motion and the parallax of the system, allowing for a precise subtraction of the kinematic contribution to the observed orbital decay. This led to a determination of the intrinsic $\dot{P}_b^{\rm int} = -25.9 \pm 3.2 \times 10^{-15}$, to be compared with the prediction of general relativity $\dot{P}_b^{\rm GR} = -27.7^{+1.5}_{-1.9} \times 10^{-15}$ (the latter prediction relies on the values of the mass of the WD and of the pulsar, obtained from optical photometry and spectroscopy [36]). The nice agreement between the two values introduces a very strong upper limit on *dipolar* gravitational wave emission, which is reflected on the diagram of Figure 5.

Finally, it is worth noting also the rejection of any model with $\beta_0 \lesssim -5$ which is imposed by J1141−6545, J1738+0333, as well as by B1534+12, J0737−3039,

and B1913+16 systems. This is a pure strong-field effect (e.g [117]), which can be exploited only using the radio pulsars, while the investigation of such low negative values of β_0 is escaping all the Solar System experiments.

Additional constraints on deviations from GR due to strong self-field effects derive from the discovery at the Green Bank radio telescope (reported by [118, 119] during 2013), and the subsequent radio timing and optical observations, of the J0348+0432 system [6]. It includes a white dwarf and a massive pulsar (2.01 ± 0.04 $M_\odot$) in a 2.46 hr almost circular orbit. Given its large mass, PSR J0348+0432 has a gravitational binding energy $\sim 60\%$ larger than that of all the other known pulsars with a measured orbital decay (the highest mass of which is $1.46^{+0.06}_{-0.05}$ $M_\odot$ for PSR J1738+0333), and the self-field effects (scaling nonlinearly with the binding energy) are expected to be much more prominent in this binary than in the ones described above. Therefore, the consistency (at the 18% level at the time being [6]) of the observed orbital decay with the predictions of GR can be used [6] to pose stringent limits to the occurrence of strong-field deviations from the Einsteinian theory in the form of a long-range field[7].

5 Perspectives

As anticipated in the previous sections, a wealth of improved/new tests of gravity theories is expected to emerge from keeping on observing the already known systems, both with the current generation or with new timing instruments, like MeerKAT (in South-Africa) and/or the Large European Array for Pulsars (LEAP), which combines the five largest European radio telescopes to generate the equivalent of a $\sim$ 200-m dish [120]. Other relativistic [pulsar+neutron star] or [pulsar+white dwarf] binaries should also be discovered by the ongoing large search experiments, at Parkes [121], Green Bank [122], Arecibo [123] and Effelsberg radio telescopes, all of them having better sensitivity than all previous surveys. Targeted searches towards gamma-ray point sources [124] have also already demonstrated to be a new promising channel for unveiling recycled pulsars, some of them likely included in relativistic binaries.

Looking on a longer decennial time-scale, the perspectives in this field of research will undergo a new gigantic step forward when novel large instruments, like the Square Kilometer Array (SKA) [125] or the Five-hundred meter A-spherical Single-aperture radio Telescope (FAST) [126] will enter in operation. In particular, they will almost certainly lead to the discovery of some [pulsar+black hole] binaries, the long-dreamt and still unsatisfied objective of all the current pulsar search collaborations. These binaries are expected to be very rare, but, besides the most obvious case of a pulsar orbiting the super-massive black hole in the Galactic centre ([127] and references therein), at least some pulsars should be found with a stellar-mass black hole companion (e.g. [128]) and, even more interestingly, some recycled

[7] Obviously, short range fields, not affecting the binary dynamics, cannot be constrained with this kind of tests.

pulsars could be discovered in a globular cluster orbiting an intermediate mass black hole [129].

Timing a natural clock orbiting a spinning black hole will give the unprecedented possibility of a direct measurement not only of the mass of the black hole $M_{\rm BH}$, but also of its angular momentum $S_{\rm BH}$ and its quadrupole moment $Q_{\rm BH}$, thus in turn allowing one to experimentally test [130, 131] the so-called *Cosmic Censorship Conjecture* [132], and the *No-Hair Theorem*. The first states that no-naked singularity (i.e. a singularity not hidden behind an event horizon) exists, while the second affirms that any black hole can be described only on the basis of $M_{\rm BH}, S_{\rm BH}$, and its electric charge, the latter not being usually relevant in an astrophysical context. Since the event horizon tends to shrink as a black hole spins up, the *Cosmic Censorship Conjecture* implies that there is a maximum spin for a black hole of a given mass; on the other hand the *No-Hair Theorem* requires that $Q_{\rm BH}$ must be expressed in terms of $M_{\rm BH}$ and $S_{\rm BH}$. Introducing the dimensionless spin and quadrupole parameters χ and q,

$$\chi = \frac{c}{G}\frac{S_{\rm BH}}{M_{\rm BH}^2} \;\; ; \;\; q = \frac{c^4}{G^2}\frac{Q_{\rm BH}}{M_{\rm BH}^3} \tag{20}$$

one then expects a black hole to satisfy in general relativity the equations

$$\chi \leq 1 \;\; ; \;\; q = -\chi^2 \tag{21}$$

which can be experimentally checked with the timing of a [pulsar+black hole] binary.

Although it is not within the scope of this review, it is worth concluding by briefly recalling the very promising expectations of the so-called *Pulsar Timing Arrays* for tests of gravitational theories [133]. They are based on the consideration of the Earth and a pulsar as a pair of test masses in the space-time metric; the passage of a gravitational wave perturbs the metric and is then expected to leave a signature on the observed timing residuals of the pulsar. The size of the effect on the residuals is very small and is proportional to the amplitude of the characteristic strain (see the chapter by Braccini & Fidecaro in this book for an introduction to the gravitational waves and a description of their basic parameters). The correlation between the data of many Earth-pulsar pairs [134] distributed throughout the sky (thus forming a PTA) is required to remove spurious effects on the timing residuals and lead to a significant detection of gravitational waves. In particular, the PTAs are most sensitive to gravitational waves with periods $\gtrsim 1$ year (i.e. frequency $\lesssim 10$ nHz), and therefore probe the nanoHertz gravitational wave sky, thus being nicely complementary to the other experiments aimed at a direct detection of gravitational waves (like LIGO/VIRGO, Advanced LIGO/VIRGO, eLISA and CMB-POL), all operating in other frequency bands. The most suitable target for the current PTAs [the Australian one (PPTA; [135]), the European one (EPTA, embedding the aforementioned LEAP experiment; [136]), and the US-Canadian one (nanoGrav; [137])], as well as for the international joined effort, labelled IPTA [138], is the stochastic background – or better saying the stocastic *foreground* – of gravitational waves produced by coalescing super-massive black hole binaries in the early stage of assembling

of the galaxies (red-shift ~ 1) in the universe. Although no claim for a detection has been announced so far by the various involved groups (the most updated upper limits are reported in [139, 140, 141]), the present trend in the timing accuracy of the experiments and the calculation of the cosmological models lend support to the possibility of a clear detection within a few years [142, 143, 139]. Since most metric gravitational theories (e.g. all of those which are Lorentz-invariant) unavoidably predict emission of waves from coalescing binaries [144], it would be very surprising (and would determine a revolution in physics or in cosmology) if not only the current instruments, but also SKA and FAST will fail to detect the aforementioned foreground. What seems more likely is that the superb sensitivity of SKA and FAST will not only lead to a simple detection, but will give the chance of using the properties of the observed gravitational waves for constraining the alternate gravity theories (e.g. by studying the mass and the spin of the gravitons [145]), as well as for characterizing the parameters of the massive black hole binary systems (e.g. [146, 147]).

With all these exciting perspectives, pulsar science is more vital than ever and promises to give additional fundamental contributions to our understanding of fundamental physics and relativistic gravity just on the eve of its first half-century.

Acknowledgements AP and MB received support for this review under the program *Progetti per Ricerca di Base 2010* of Regione Autonoma della Sardegna (L.R. 7/2007). AP and MB acknowledge the collaborators at INAF-Osservatorio di Cagliari and the people all around the world which are contributing to make the study of the pulsars an always stimulating and often surprising activity. In particular P. Esposito for having carefully read an early version of this manuscript, giving useful suggestions for making it handier for the neophytes of this field of research.

References

1. J. M. Cordes & T. J. W. Lazio, *NE2001. I. A New Model for the Galactic Distribution of Free Electrons and its Fluctuations*, **arXiv:astro-ph/0207156** (2002)
2. J. L. Han, R. N. Manchester, A. G. Lyne, G. J. Qiao & W. van Straten, *Pulsar rotation measures and the large-scale structure of the galactic magnetic field*, *ApJ*, **642**, 868–881 (2006)
3. M. Colpi, A. Possenti & A. Gualandris *The Case of PSR J1911-5958A in the Outskirts of NGC 6752: Signature of a Black Hole Binary in the Cluster Core?*, *ApJ*, **570**, L85–L88 (2002)
4. J.W.T. Hessels, *et al A Radio Pulsar Spinning at 716 Hz*, *Science*, **311**, 1901 (2006)
5. P. Demorest, T. Pennucci, S. Ransom, M. Roberts & J.W.T. Hessels, *Shapiro delay measurement of a 2 solar mass neutron star*, *Nature*, **467**, 1081 (2010)
6. J. Antoniadis *et al.*, *A Massive Pulsar in a Compact Relativistic Binary*, *Science*, **340**, 1233232 (2013)
7. N. Wex, & M. Kramer, *Generic Gravity Tests with the Double Pulsar*, in Proc of the 12th Marcel Grossmann Meeting on General Relativity (MG 12), Paris **arXiv:1001.4733** (2010)
8. F. Haberl, *The magnificent seven: magnetic fields and surface temperature distributions*, *Ap&SS*, **308**, 181 (2007)
9. G.G. Pavlov, D. Sanwal & M.A. Teter. *Central Compact Objects in Supernova Remnants*, in Young Neutron Stars and Their Environments, eds. F. Camilo & B. Gaensler, *IAUS*, **218**, 239 (2004)

10. E.F. Keane& M.A. McLaughlin *Rotating radio transients*, *BASI*, **39**, 333 (2011)
11. P.M. Woods & C. Thompson *Soft gamma repeaters and anomalous X-ray pulsars: magnetar candidates*, in Compact stellar X-ray sources. Edited by Walter Lewin & Michiel van der Klis *Cambridge Astrophysics Series*, **39**, 547 – 586 (2006)
12. K. Chen & M. Ruderman, *Pulsar death lines and death valley*, *ApJ*, **402**, 264–270 (1993)
13. R. N. Manchester, G. B. Hobbs, A. Teoh & M. Hobbs, *The Australia Telescope National Facility Pulsar Catalogue*, *AJ*, **129**, 1993 (2005)
14. `http://www.atnf.csiro.au/research/pulsar/psrcat/`
15. `http://www.physics.mcgill.ca/~pulsar/magnetar/main.html`
16. M. A. Alpar, A. F. Cheng, M. A. Ruderman & J. Shaham, *A new class of radio pulsars*, *Nature*, **300**, 728–730 (1982)
17. F. Verbunt, *Origin and evolution of X-ray binaries and binary radio pulsars*, *Ann. Rev. Astr. Ap.*, **31**, 93 (1993)
18. P. Podsiadlowski, *Electron-capture Supernovae and Accretion-induced Collapse of ONeMg White Dwarfs*, in "Paths to Exploding Stars: Accretion and Eruption", KITP conference: march 2007, Kavli Institute, Santa Barbara (2007)
19. S. Rappaport, E. Pfahl, F. A. Rasio & P. Podsiadlowski, *Formation of Compact Binaries in Globular Clusters*, in P. Podsiadlowski, S. Rappaport, A. R. King, F. D'Antona, & L. Burderi (eds.), Evolution of Binary and Multiple Star Systems, **229**, ASP Conf. Ser., 409 (2001)
20. S.B. Popov, J.A. Pons, J.A. Miralles, P.A. Boldin, B. Posselt *Population synthesis studies of isolated neutron stars with magnetic field decay*, *MNRAS*, **401** 2675 (2010)
21. C-A. Faucher-Giguère & V.M. Kaspi, *Birth and Evolution of Isolated Radio Pulsars*, *ApJ*, **643** 332 (2006)
22. M. Burgay *et al.*, *An increased estimate of the merger rate of double neutron stars from observations of a highly relativistic system*, *Nature*, **426**, 531–533 (2003)
23. A. G. Lyne *et al.*, *A double-pulsar system: A rare laboratory for relativistic gravity and plasma physics*. *Science*, **303**, 1153–1157 (2004)
24. D. J. Nice, R. W. Sayer & J. H. Taylor, *PSR J1518+4904: A mildly relativistic binary pulsar system*, *ApJ*, **466**, L87–L90 (1996)
25. A. Wolszczan, *PSR 1257+12 and PSR 1534+12*, IAU Circ., 5073, 1, Edited by Green, D. W. E. (1990)
26. I. H. Stairs *et al.*, *Measurement of relativistic orbital decay in the PSR B1534+12 binary system*, *ApJ*, **505**, 352–357 (1998)
27. A. J. Faulkner *et al.*, *PSR J1756−2251: A new relativistic double neutron star system*, *ApJ*, **618**, L119–L122 (2005)
28. A. G. Lyne *et al.*, *The Parkes multibeam pulsar survey: PSR J1811−1736 – a pulsar in a highly eccentric binary system*, *MNRAS*, **312**, 698–702 (2000)
29. A. Corongiu *et al.*, *The binary pulsar PSR J1811−1736: evidence of a low amplitude supernova kick*, *A&A*, **462**, 703–709 (2007)
30. D. J. Champion *et al.*, *PSR J1829+2456: a relativistic binary pulsar*, *MNRAS*, **350**, L61–L65 (2004)
31. D. R. Lorimer *et al.*, *Arecibo Pulsar Survey Using ALFA. II. The Young, Highly Relativistic Binary Pulsar J1906+0746*, *ApJ*, **640**, 428–434 (2006)
32. R. A. Hulse & J. H. Taylor, *Discovery of a pulsar in a binary system*, *ApJ*, **195**, L51–L53 (1975)
33. J. M. Weisberg & J. H. Taylor, *The Relativistic Binary Pulsar B1913+16*, in Bailes, M., Nice, D. J. & Thorsett, S. (eds.) Radio Pulsars, 93–98 Astronomical Society of the Pacific, San Francisco, (2003)
34. S. B. Anderson, P. W. Gorham, S. R. Kulkarni & T. A. Prince, *Discovery of two radio pulsars in the globular cluster M15*, *Nature*, **346**, 42–44 (1990)
35. B. A. Jacoby *et al.*, *Measurement of Orbital Decay in the Double Neutron Star Binary PSR B2127+11C*, *ApJ*, **644**, L113–L116 (2006)
36. J. Antoniadis, M.H. van Kerkwijk, D. Koester, *et al.*, *The relativistic pulsar-white dwarf binary PSR J1738+0333 - I. Mass determination and evolutionary history*, *MNRAS*, **423** 3316 (2012)

37. P.P.C. Freire, N. Wex, G. Esposito-Farese, *et al.*, *The relativistic pulsar-white dwarf binary PSR J1738+0333 - II. The most stringent test of scalar-tensor gravity*, *MNRAS*, **423**, 3328 (2012)
38. S. M. Ransom, I.H. Stairs, A.M. Archibald *et al*, *A millisecond pulsar in a stellar triple system*, *Nature*, in press (2014)
39. T. Tauris & E. van den Heuvel, *Formation of the Galactic Millisecond Pulsar Triple System PSR J0337+1715A Neutron Star with Two Orbiting White Dwarfs*, *ApJ*, **781**, L13 (2014)
40. D.R. Lorimer & M. Kramer, in *Handbook of Pulsar Astronomy*, Cambridge University Press, Cambridge (2005)
41. A.G. Lyne & G. Smith, in *Pulsar Astronomy*, 3rd ed., Cambridge University Press, Cambridge (2005)
42. R.N. Manchester & J.H. Taylor, in *Pulsars*, Freeman & Co., San Francisco (1977)
43. E.g. `http://ssd.jpl.nasa.gov/?planet_eph_export`
44. E.g. `http://www.iers.org/IERS/EN/Publications/Bulletins/bulletins.html`
45. Shapiro, I. I., *Fourth Test of General Relativity*, *Phys. Rev. Lett.* **13**, 789 (1964)
46. W. van Straten, M. Bailes, M. Britton, S.R. Kulkarni, S.B. Anderson, R.N. Manchester, J. Sarkissian, *A test of general relativity from the three-dimensional orbital geometry of a binary pulsar*, *Nature*, **412** 158
47. P.W. Anderson, & N.Itoh, *Pulsar glitches and restlessness as a hard superfluidity phenomenon*, *Nature*, **256**, 25 (1975)
48. M.A., Alpar, R., Nandkumar, D. Pines, , *ApJ*, **311**, 197 (1986)
49. T.V. Shabanova, *Slow glitches in the pulsar B1822-09*, *Astrophys. Space Sci.*, **308**, 591 (2007)
50. A.G. Lyne, G. Hobbs, M. Kramer, I. Stairs, B. Stappers, *Switched Magnetospheric Regulation of Pulsar Spin-Down*, *Science*, **329**, 408 (2010)
51. G. Hobbs, A.G. Lyne, M. Kramer, *An analysis of the timing irregularities for 366 pulsars*, *MNRAS*, **402**, 1027 (2010)
52. I. Cognard, & D.C. Backer, *A Microglitch in the Millisecond Pulsar PSR B1821-24 in M28*, *ApJ*, **612**, 125 (2004)
53. R.M. Shannon & J.M. Cordes, *Assessing the role of spin noise in the precision timing of millisecond pulsars*, *ApJ*, **725**, 1607 (2010)
54. C. Will, in *Theory and Experiments in Gravitational Physics*, Cambridge University Press, Cambridge (1993)
55. C. Will, *The Confrontation between General Relativity and Experiment* in *General Relativity and John Archibald Wheeler*, eds I. Ciufolini and R.A. Matzner, ASSL **367**, 73 (2010)
56. T. Damour, and G. Esposito-Farèse, *Testing gravity to second post-Newtonian order: A field-theory approach*, *Phys. Rev. D.*, **53**, 5541 (1996)
57. C. Will, *The Confrontation between General Relativity and Experiment*, LLR `http://relativity.livingreviews.org/Articles`, **9**, 3 (2006)
58. C. Will, & K.J. Nordvedt, *Conservation Laws and Preferred Frames in Relativistic Gravity. I. Preferred-Frame Theories and an Extended PPN Formalism*, *ApJ*, **177**, 757 (1972)
59. T. Damour, and G. Esposito-Farèse, *Tensor-multi-scalar theories of gravitation* , *Class. Quantum Grav.*, **9**, 2093 (1992)
60. I. Stairs, *Testing General Relativity with Pulsar Timing*, LLR `http://relativity.livingreviews.org/Articles`, **6**, 5 (2003)
61. K. Nordtvedt, *Testing Relativity with Laser Ranging of the Moon*, *Phys. Rev.*, **170**, 1186 (1968)
62. I. H. Stairs *et al.*, *Discovery of three wide-orbit binary pulsars: implications for binary evolution and equivalence principles*, *ApJ*, **632**, 1060 (2005)
63. M.E. Gonzales, *al.*, *High-precision Timing of Five Millisecond Pulsars: Space Velocities, Binary Evolution and Equivalence Principles*, *Astrophys. J.*, **743**, 102 (2011)
64. T. Damour & G. Schäfer, *New tests of the strong equivalence principle using binary pulsar data*, *Phys. Rev. Lett.*, **66**, 2549, (1991)
65. P.C.C. Freire, M. Kramer, N. Wex, *Tests of the universality of free fall for strongly self-gravitating bodies with radio pulsars*, *Classical and Quantum Gravity*, **29**, 184007 (2012)

66. L. Shao & N. Wex, *New tests of local Lorentz invariance of gravity with small-eccentricity binary pulsars*, *Classical and Quantum Gravity*, **29**, 215018 (2012)
67. L. Shao, R. N. Caballero, M. Kramer *et al.*, *A new limit on local Lorentz invariance violation of gravity from solitary pulsars*, *Classical and Quantum Gravity*, **30**, 165019 (2013)
68. J. Müller, J. G. Williams, & S. G. Turyshev, *Lunar laser ranging contributions to relativity and geodesy*, in H. Dittus, C. Lammerzahl & S. G. Turyshev eds, *Lasers, Clocks and Drag-Free Control: Exploration of Relativistic Gravity in Space*, *Astrophysics and Space Science Library*, **349**, 457 (2008)
69. K. Nordtvedt, *Probing gravity to the second post-Newtonian order and to one part in 107 using the spin axis of the sun*, *ApJ*, **320**, 871 (1987)
70. , L. Shao, N. Wex, *New limits on the violation of local position invariance of gravity*, *Classical and Quantum Gravity*, **30**, 165020 (2013)
71. R. J. Warburton & J. M. Goodkind. *Search for evidence of a preferred reference frame*, *ApJ*, **208**, 881 (1976)
72. C.M. Will, *Is momentum conserved? A test in the binary system PSR B1913+16*, *ApJ*, **393**, L59 (1992)
73. T. Damour & N. Deruelle, *General relativistic celestial mechanics of binary systems. I. The post-Newtonian motion.*, *Ann. Inst. H. Poincaré (Phys. Théor.)* **43**, 107 (1985)
74. T. Damour & N. Deruelle, *General relativistic celestial mechanics of binary systems. II. The post-Newtonian timing formula.*, *Ann. Inst. H. Poincaré (Phys. Théor.)* **44**, 263 (1986)
75. J.H. Taylor, & J. M. Weisberg, *Further experimental tests of relativistic gravity using the binary pulsar PSR 1913+16*, *ApJ*, **345**, 434 (1989)
76. T. Damour,& J.H. Taylor, *Strong-field tests of relativistic gravity and binary pulsars*, *Phys. Rev. D*, **45**, 1840 (1992)
77. R.A. Hulse, & J.H. Taylor, *Discovery of a pulsar in a binary system*, *ApJ*, **195**, L51 (1975)
78. J.M. Weisberg, D.J. Nice & J.H. Taylor, *Timing Measurements of the Relativistic Binary Pulsar PSR B1913+16*, *ApJ*, **722**, 1030 (2010)
79. T. Damour, *The problem of motion in Newtonian and Einsteinian gravity*, in *Three Hundred Years of Gravitation*, eds S.W. Hawking, W. Israel, (Cambridge Univ. Press, Cambridge, 128 (1987)
80. T. Damour,& J.H. Taylor, *On the orbital period change of the Binary Pulsar PSR 1913+13*, *ApJ*, **366**, 501 (1991)
81. A. Wolszczan, *A nearby 37.9 ms radio pulsar in a relativistic binary system*, *Nature*, **350**, 688 (1991)
82. I.H. Stairs, S.E. Thorsett, J.H. Taylor, A. Wolszczan, *Studies of the relativistic binary pulsar PSR B1534+12: I. Timing Analysis*, *ApJ*, **581**, 501 (2002)
83. M. Burgay, *et al.*, *The Parkes high latitude pulsar survey*, *MNRAS*, **368** 283 (2006)
84. V. Kalogera, *et al.*, *The Cosmic Coalescence Rates for Double Neutron Star Binaries ApJ*, **601**, L179 (2004)
85. L. Stella, & A. Possenti, *Lense-Thirring precession in the Astrophysical Context*, *Space Sci.Rev.*, **148**, 105 (2009)
86. R.P. Breton, *et al.*, *Relativistic Spin Precession in the Double Pulsar*, *Science*, **321**, 104 (2008)
87. B.M. Barker, & R.F. O'Connell, *Gravitational two-body problem with arbitrary masses, spins, and quadrupole moments* , *Phys. Rev. D* **12**, 329 (1975)
88. I. H. Stairs, S. E. Thorsett & Z. Arzoumanian, *Measurement of Gravitational Spin-Orbit Coupling in a Binary-Pulsar System*, *Phys. Rev. Lett.*, **93**, 141101 (2004)
89. M. Kramer *Determination of the Geometry of the PSR B1913+16 System by Geodetic Precession*, *ApJ*, **509**, 856 (1998)
90. J.M. Weisberg, & J.H. Taylor, *General Relativistic Geodetic Spin Precession in Binary Pulsar B1913+16: Mapping the Emission Beam in Two Dimensions*, *ApJ*, **576** 942 (2002)
91. T. Clifton, & J.M. Weisberg, *A Simple Model for Pulse Profiles from Precessing Pulsars, with Special Application to Relativistic Binary PSR B1913+16*, *ApJ*, **679**, 687 (2008)
92. R.N. Manchester, *et al.*, *Observations and Modeling of Relativistic Spin Precession in PSR J1141-6545*, *ApJ*, **710** 1694 (2010)

93. R.N. Manchester, *et al.*, *The Mean Pulse Profile of PSR J0737-3039A, ApJ* **621**, 49 (2005)
94. R.D. Ferdman, *et al.*, *The double pulsar: evolutionary constraints from the system geometry*, in *40 years of pulsars*. AIP Conf Proc, **983** 474 (2008)
95. M. Kramer, & I. Stairs, *The Double Pulsar, Ann. Rev. A&A*, **46**, 541 (2008)
96. M. Kramer, *et al.*, *Tests of General Relativity from Timing the Double Pulsar*, *Science*, **314**, 97 (2006)
97. B.B.P. Perera, *et al.*, *The evolution of PSR J0737−3039B and a model for relativistic spin precession*, *ApJ*, **721**, 1193 (2010)
98. A.T. Deller, M. Bailes, S.J. Tingay, *Implications of a VLBI Distance to the Double Pulsar J0737-3039A/B*, *Science*, **323**, 1327 (2009)
99. N. Wex, & M. Kramer, *A characteristic observable signature of preferred-frame effects in relativistic binary pulsars*, *MNRAS*, **380**, 455 (2007)
100. T. Damour, & G. Schaefer, *Higher-order relativistic periastron advances and binary pulsars*, *Nuovo Cim.*, **101**, 127 (1988)
101. J.M. Lattimer, B.F. Schutz, *Constraining the Equation of State with Moment of Inertia Measurements*, *ApJ*, **629** 979 (2005)
102. S. Johnston, *et al.*, *Discovery of a very bright, nearby binary millisecond pulsar*, *Nature*, **361**, 613 (1993)
103. A. Deller, S.J. Tingay, M. Bailes, J.E. Reynolds, *Precision Southern Hemisphere VLBI Pulsar Astrometry. II. Measurement of Seven Parallaxes*, *ApJ*, **701**, 1243 (2009)
104. S.M. Kopeikin, *On possible implications of orbital parallaxes of wide orbit binary pulsars and their measurability*, *ApJ*, **439**, L5, (1995)
105. S.M. Kopeikin, *Proper motion of binary pulsars as a source of secular variation of orbital parameters*, *ApJ*, **467**, L93 (1996)
106. W. van Stratten, *et al.*, *A test of general relativity from the three-dimensional orbital geometry of a binary pulsar*, *Nature*, **412**, 158 (2001)
107. J. Verbiest, *et al.*, *Precision Timing of PSR J0437-4715: An Accurate Pulsar Distance, a High Pulsar Mass, and a Limit on the Variation of Newton's Gravitational Constant*, *ApJ*, **679**, 675 (2008)
108. V. M. Kaspi *et al.*, *Discovery of a young radio pulsar in a relativistic binary orbit*, *ApJ*, **543**, 321–327 (2000)
109. J. Antoniadis, C.G. Bassa, N. Wex, M. Kramer, R. Napiwotzki, , *MNRAS*, **412**, 580 (2011)
110. T. M. Tauris and T. Sennels, *Formation of the binary pulsars PSR B2303+46 and PSR J1141-6545. Young neutron stars with old white dwarf companions*, *A&A*, **355**, 236 (2000)
111. N.D.R. Bhat, M. Bailes, & J.P.W. Verbiest, *Gravitational-radiation losses from the pulsar white-dwarf binary PSR J1141 6545*, *Phys. Rev. D*, **77.12**, 124017 (2008)
112. T. Damour, and G. Esposito-Farèse, *Tensor-scalar gravity and binary pulsar experiments*, *Phys. Rev. D.*, **54**, 1474 (1996)
113. C. Brans & R.H. Dicke, *Mach's Principle and a Relativistic Theory of Gravitation*, *Phys. Rev.*, **124**, 925 (1961)
114. C.M. Will & H.W. Zaglauer, *Gravitational radiation, close binary systems, and the Brans-Dicke theory of gravity*, *ApJ*, **346**, 366 (1989)
115. G. Esposito-Farèse, *Binary-Pulsars tests of strong-field gravity and gravitational radiation damping*, in proceed. of *X Marcel Grossman meeting*, Rio de Janeiro, July 2003, p. 647 (2005)
116. B.A. Jacoby, Ph.D. Thesis at *California Institute of Technology:* California - USA, Publication Number: AAT **3161140** (2005)
117. G. Esposito-Farèse, *Motion in alternative theories of gravity*, lecture given at *School on Mass*, Orléans (France), June 2008, Arxiv:0905.2575 (2009)
118. J. Boyles *et al.*, *The Green Bank Telescope 350 MHz drift-scan survey. I. Survey observations and the discovery of 13 pulsars*, *Astrophys. J.*, **763**, 80 (2013).
119. R. S. Lynch *et al.*, *The Green Bank Telescope 350 MHz drift-scan survey. II: Data analysis and the timing of 10 new pulsars, including a relativistic binary*, *Astrophys. J.*, **763**, 81 (2013)
120. R.D. Ferdman, *et al.*, *The European Pulsar Timing Array: current efforts and a LEAP toward the future*, *Class.Quant.Gr.*, **27** 084014 (2010)

121. M.J. Keith, *et al.*, *The High Time Resolution Universe Pulsar Survey I: System configuration and initial discoveries*, *MNRAS*, **409**, 619 (2010)
122. J. Boyles, *et al.*, *Timing Derived Properties Of The First Discoveries From The GBT 350-MHz Pulsar Survey*, Bull. of the AAS, **42**, 464 (2010)
123. M. Beroiz, *et al.*, *Current Results at PALFA Pulsar Survey at Arecibo Observatory*, Bull. of the AAS, **42**, 460 (2010)
124. A.A. Abdo, *et al.*, *Detection of 16 Gamma-Ray Pulsars Through Blind Frequency Searches Using the Fermi LAT*, *Science*, **325**, 840 (2009)
125. R. Smits, *Pulsar searches and timing with the square kilometre array* , *A&A*, **493** 1161 (2009)
126. R. Smits, *Pulsar science with the Five hundred metre Aperture Spherical Telescope*, *A&A*, **506** 919 (2009)
127. I.S. Deneva, in *Elusive neutron star populations: Galactic center and intermittent pulsars*, Ph.D. dissertation, Cornell Univ, USA (2010)
128. E. Pfahl, P. Podsiadlowski, S. Rappaport, *Relativistic Binary Pulsars with Black Hole Companions*, *ApJ*, **628**, 343 (2005)
129. B. Devecchi, M. Colpi, M. Mapelli, A. Possenti, *Millisecond pulsars around intermediate-mass black holes in globular clusters*, *MNRAS*, **380**, 691 (2007)
130. M. Kramer, *et al.*, *Strong-field tests of gravity using pulsars and black holes*, *New Astr. Rev.*, **48**, 993 (2004)
131. K. Liu, N. Wex, M. Kramer, J.M. Cordes, T.J.W. Lazio, *Prospects for Probing the Spacetime of Sgr A* with Pulsars*, *ApJ*, **747**, L1 (2012)
132. S.W. Hawking, & R. Penrose, *The Singularities of Gravitational Collapse and Cosmology*, in *Royal Soc. Proceed. Ser. A*, **314**, 529 (1970)
133. R. Foster & D. Backer, *Constructing a pulsar timing array*, *ApJ*, **361**, 300 (1990)
134. R. Hellings & G. Downs,*Upper limits on the isotropic gravitational radiation background from pulsar timing analysis*, *ApJ*, **265** L39 (1983)
135. G. Hobbs, *The Parkes Pulsar Timing Array*, *Classical and Quantum Gravity*, **30**, 224007, (2013)
136. M. Kramer & D. Champion , *The European Pulsar Timing Array and the Large European Array for Pulsars*, *Classical and Quantum Gravity*, **30**, 224009, (2013)
137. M.A. McLaughlin, *The North American Nanohertz Observatory for Gravitational Waves*, *Classical and Quantum Gravity*, **30**, 224008, (2013)
138. G. Hobbs *et al.*, *The International Pulsar Timing Array project: using pulsars as a gravitational wave detector*, *Classical and Quantum Gravity*, **27**, 084013, (2010)
139. R. van Haasteren, *et al.*, *Placing limits on the stocastic gravitational-wave background using European Timing Array data*, *MNRAS*, **414** 3117 (2011)
140. P.B. Demorest *et al.*, *Limits on the Stochastic Gravitational Wave Background from the North American Nanohertz Observatory for Gravitational Waves*, *ApJ*, **762**, 94 (2013)
141. R. Shannon *et al.*, *Gravitational-wave limits from pulsar timing constrain supermassive black hole evolution*, *Science*, **342**, 334 (2013)
142. J. Verbiest, *et al.*, *Timing stability of millisecond pulsars and prospects for gravitational-wave detection MNRAS*, **400**, 951 (2009)
143. D.R.B. Yardley, *et al.*, *The Sensitivity of the Parkes Pulsar Timing Array to Individual Sources of Gravitational Waves*, *MNRAS*, **407**, 669 (2010)
144. K.S. Thorne, *Multipole expansions of gravitational radiation*, *Rev. Modern Phys.*, **52**, 299 (1980)
145. K. Lee, *et al.*, *Detecting massive gravitons using pulsar timing arrays*, *ApJ*, **722** 1589 (2010)
146. A. Sesana, & A.Vecchio, *Measuring the parameters of massive black hole binary systems with pulsar timing array observations of gravitational waves*, *Phys. Rev. D*, **81**, 104008 (2010)
147. X. Deng & L.S. Finn, *Pulsar timing array observations of gravitational wave source timing parallax*, *MNRAS*, **414** 50 (2011)